NAVAL POSTGRADUATE SCHOOL

MONTEREY, CALIFORNIA

THESIS

INDUSTRIAL CONTROL OF A SUPERCAPACITOR AND COMPRESSED AIR STORAGE SYSTEM

by

Han Qi Alvin Tan

March 2019

Thesis Advisor: Anthony J. Gannon
Co-Advisor: Andrea D. Holmes

Approved for public release. Distribution is unlimited.

THIS PAGE INTENTIONALLY LEFT BLANK

1. AGENCY USE ONLY *(Leave blank)*	**2. REPORT DATE** March 2019	**3. REPORT TYPE AND DATES COVERED** Master's thesis	
4. TITLE AND SUBTITLE INDUSTRIAL CONTROL OF A SUPERCAPACITOR AND COMPRESSED AIR STORAGE SYSTEM			**5. FUNDING NUMBERS**
6. AUTHOR(S) Han Qi Alvin Tan			
7. PERFORMING ORGANIZATION NAME(S) AND ADDRESS(ES) Naval Postgraduate School Monterey, CA 93943-5000			**8. PERFORMING ORGANIZATION REPORT NUMBER**
9. SPONSORING / MONITORING AGENCY NAME(S) AND ADDRESS(ES) N/A			**10. SPONSORING / MONITORING AGENCY REPORT NUMBER**
11. SUPPLEMENTARY NOTES The views expressed in this thesis are those of the author and do not reflect the official policy or position of the Department of Defense or the U.S. Government.			
12a. DISTRIBUTION / AVAILABILITY STATEMENT Approved for public release. Distribution is unlimited.			**12b. DISTRIBUTION CODE** A

13. ABSTRACT (maximum 200 words)

For fiscal year 2017, according to the Department of Energy's June 2018 sustainability performance report, the DoD's total energy consumption stood at 210 quadrillion joules (199 trillion Btu) of energy with a total energy expenditure of $11.9 billion. The majority of its energy budget was spent on the purchase of fossil fuels. This reliance on fossil fuels to sustain military operations would pose serious financial, operational, and strategic challenges and risks to the energy security and resiliency of the military. To reduce the reliance on fossil fuels, SECNAV has set forth five energy goals as key steps for the Navy to switch to alternative renewable energy sources.

This thesis focuses on the design and development of a feasible micro-grid powered by renewable energy to fulfil SECNAV's energy goal of increasing alternative energy ashore by producing 50% of shore-based energy requirements from alternative sources by 2020.

The main aim of the thesis is to design and provide a proof of concept for an automated industrial control of a supercapacitor microgrid and compressed air storage system by integrating an alternate power supply in the supercapacitor solar microgrid and compressed air storage system, and by designing an algorithm to control the power supply using off-the-shelf automated industrial components.

14. SUBJECT TERMS supercapacitor, compressed air, microgrid			**15. NUMBER OF PAGES** 111
			16. PRICE CODE
17. SECURITY CLASSIFICATION OF REPORT Unclassified	**18. SECURITY CLASSIFICATION OF THIS PAGE** Unclassified	**19. SECURITY CLASSIFICATION OF ABSTRACT** Unclassified	**20. LIMITATION OF ABSTRACT** UU

i

THIS PAGE INTENTIONALLY LEFT BLANK

INDUSTRIAL CONTROL OF A SUPERCAPACITOR AND COMPRESSED AIR STORAGE SYSTEM

Han Qi Alvin Tan
Major, Republic of Singapore Navy
BSE, National University of Singapore, 2006

Submitted in partial fulfillment of the
requirements for the degree of

MASTER OF SCIENCE IN MECHANICAL ENGINEERING

from the

NAVAL POSTGRADUATE SCHOOL
March 2019

Approved by: Anthony J. Gannon
              Advisor

              Andrea D. Holmes
              Co-Advisor

              Garth V. Hobson
              Chair, Department of Mechanical and Aerospace Engineering

THIS PAGE INTENTIONALLY LEFT BLANK

ABSTRACT

For fiscal year 2017, according to the Department of Energy's June 2018 sustainability performance report, the DoD's total energy consumption stood at 210 quadrillion joules (199 trillion Btu) of energy with a total energy expenditure of $11.9 billion. The majority of its energy budget was spent on the purchase of fossil fuels. This reliance on fossil fuels to sustain military operations would pose serious financial, operational, and strategic challenges and risks to the energy security and resiliency of the military. To reduce the reliance on fossil fuels, SECNAV has set forth five energy goals as key steps for the Navy to switch to alternative renewable energy sources.

This thesis focuses on the design and development of a feasible micro-grid powered by renewable energy to fulfil SECNAV's energy goal of increasing alternative energy ashore by producing 50% of shore-based energy requirements from alternative sources by 2020.

The main aim of the thesis is to design and provide a proof of concept for an automated industrial control of a supercapacitor microgrid and compressed air storage system by integrating an alternate power supply in the supercapacitor solar microgrid and compressed air storage system, and by designing an algorithm to control the power supply using off-the-shelf automated industrial components.

THIS PAGE INTENTIONALLY LEFT BLANK

TABLE OF CONTENTS

LIST OF FIGURES

THIS PAGE INTENTIONALLY LEFT BLANK

LIST OF TABLES

THIS PAGE INTENTIONALLY LEFT BLANK

LIST OF ACRONYMS AND ABBREVIATIONS

AA-CAES	Advanced Adiabatic Compressed Air Energy Storage
ABES	Advanced Battery Energy Storage
A-CAES	Adiabatic Compressed Air Energy Storage
CAES	Compressed Air Energy Storage
D-CAES	Diabatic Compressed Air Energy Storage
DoD	Department of Defense
FES	Flywheel Energy Storage
I-CAES	Isothermal Compressed Air Energy Storage
LAES	Liquid Air Energy Storage
MPPT	Maximum Power Point Tracking
NPS-IMPEL	Naval Postgraduate School Integrated Multi-Physics Energy Lab
NREL	National Renewable Energy Lab
PHS	Pumped Hydroelectric Storage
PLC	Programmable Logic Controller
PSI	Pounds of Force Per Square Inch
PV	Photovoltaic
SC-CAES	Supercritical Compressed Air Energy Storage
SECNAV	Secretary of the Navy
SS-CAES	Small Scale Compressed Air Energy Storage
SSR	Solid-State Relay
USN	United States Navy
VDC	Volts Direct Current

THIS PAGE INTENTIONALLY LEFT BLANK

ACKNOWLEDGMENTS

I would like to offer my most heartfelt gratitude and appreciation to my advisors, Dr. Anthony Gannon and Ms. Andrea Holmes, for their understanding and invaluable advice and technical assistance offered to me throughout the course of my thesis work.

THIS PAGE INTENTIONALLY LEFT BLANK

I.   INTRODUCTION

For Fiscal Year 2017, the Department of Defense (DoD) was the largest U.S. government user of energy, and her total energy consumption stood at 210 quadrillion joules (199 trillion Btu) of energy, with a total energy expenditure of $11.9 billion [1]. A key point that could also be drawn from these statistics was that the DoD spent majority of its energy budget on the purchase of fossil fuels. This suggests that the DoD relied heavily on fossil fuels to power her military operations and infrastructure.

However, this reliance on fossil fuels would pose serious financial, operational and strategic challenges and risks to the energy security and energy resiliency of the military. To overcome the above-mentioned challenges and risks posed by the reliance of fossil fuels, and to preserve the military's energy security and resiliency, the DoD would need to take key steps to switch its energy usage to alternative renewable energy sources. For the Navy, the Secretary of the Navy (SECNAV) has set forth five energy goals, as shown in Figure 1, to reduce its reliance on fossil fuels and significantly increase the use of renewable energy sources [2].

1. Energy Efficient Acquisition	Evaluation of energy factors will be mandatory when awarding contracts for systems and buildings.
2. Sail the "Great Green Fleet"	DON will demonstrate a Green Strike Group in local operations by 2012 and sail it by 2016.
3. Reduce Non-Tactical Petroleum Use	By 2015, DON will reduce petroleum use in the commercial vehicle fleet by 50%.
4. Increase Alternative Energy Ashore	By 2020, DON will produce at least 50% of shore based energy requirements from alternative sources; 50% of DON installations will be net-zero.
5. Increase Alternative Energy Use DON-Wide	By 2020, 50% of total DON energy consumption will come from alternative sources.

Figure 1.   The Secretary of the Navy's Energy Goals. Source: [2].

While renewable energy sources are positioned as the perfect alternative to fossil fuels for electrical power generation, there are challenges in the ability to harness and utilise the renewables as a stable and reliable form of energy [3]. Renewable energy sources tend to be

intermittent by nature, and the electrical power supply generated from these renewable sources would fluctuate with ambient conditions. The fluctuations in power supply would pose serious problems to the stability and reliability of the electrical power grid. To overcome the intermittency of power generation by renewables, the system would need to include electrical storage systems to store the power generation during peak ambient conditions and reserve for usage during off-peak periods.

There are currently four main electrical storage systems: (1) Pumped Hydroelectric Storage (PHS) at 23.6 GW, (2) Compressed Air Energy Storage (CAES) at 114 MW, (3) Advanced Battery Energy Storage (ABES) at 750 MW and (3) Flywheel Energy Storage (FES) at 58MW [4]. The research of this thesis focuses on a combination of CAES-Supercapacitor microgrid due to the unique feature of scalability, which would allow the CAES-Supercapacitor microgrid system to be utilised for different durations across the entire spectrum of electrical grid applications.

Specific to the interest of the thesis, the related-research work seeks to design and develop a feasible micro-grid powered by renewable energy to fulfil SECNAV's energy goal of increasing alternative energy ashore by producing 50% of shore-based energy requirements from alternative sources by 2020 [2].

The main aim of the research is to design and provide a proof-of-concept of an automated industrial control of a supercapacitor microgrid and compressed air storage system (CAES). The thesis will seek to expand on the previous research by McLaughlin [5], Prinsen [6], Vranas [7] and Williams [8]. This thesis will also incorporate the previous research on the aspects of improving energy security and energy resiliency of military buildings ashore. The primary objective of the thesis is to integrate an alternate power supply in the supercapacitor solar microgrid and compressed air storage system and design an algorithm to control the power supply using off-the-shelf automated industrial components. This work will achieve a proof-of-concept for an automated small-scale compressed air storage system (SS-CAES) based mainly on renewable energy.

II. LITERATURE REVIEW

A. THE DEPARTMENT OF DEFENSE'S ENERGY INTERESTS IN RENEWABLE ENERGY

For FY17, DoD's total energy consumption stood at 210 quadrillion joules (199 trillion Btu) of energy with a total energy expenditure of $11.9 billion [1]. By these accounts, DoD was the largest government user of energy. Figure 2 shows the breakdown of the DoD total energy consumption by fuel type and it was apparent that the military operations relied heavily on fossil fuels and DoD spent majority of the energy budget on the purchase of fossil fuels.
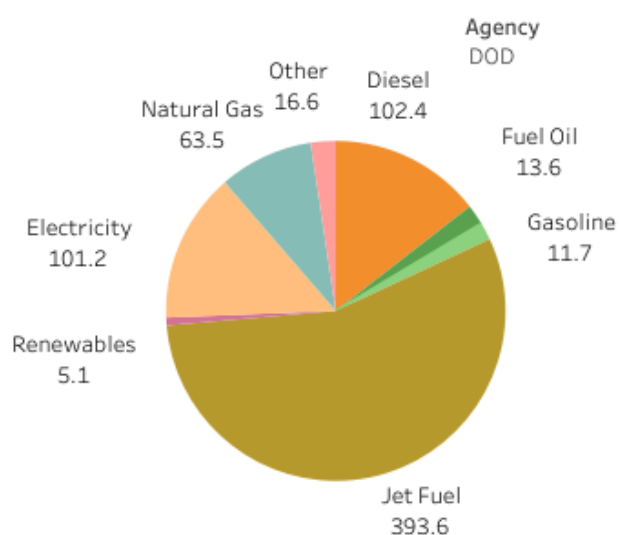
Figure 2.   DoD Total Energy Consumption 2017. Source: [1].

However, this reliance on fossil fuels would pose serious financial, operational and strategic challenges and risks to the energy security and energy resiliency of the military:

- Financial challenges and risks would refer to the longer-term trend of rising cost of fuel and shorter-term volatility in fuel prices.

- Operational challenges and risks would refer to the vulnerability of fuel supply lines to disruption and sabotage.

- Strategic challenges and risks would refer to the continual efforts to ensure access to fuel globally so that fuel can be supplied to the forward deployed area.

To overcome the above-mentioned challenges and risks posed by the reliance of fossil fuels, the military would need to take key steps to switch its own energy usage to the more efficient renewable energy sources. For the Navy, the Secretary of the Navy (SECNAV) set forth five energy goals to reduce the military's reliance on fossil fuels and significantly increase the use of renewable energy sources.

Parallel to DoD's interest in renewable energies to improve the military energy security and resiliency, there had also been heightened public interest and capital investments in renewables which drove exponential growth in renewable energy researches and projects. The increase in renewable-related researches and projects would increase the knowledge banks and drive economies of scale in production cost. This would greatly benefit the DoD's transition from fossil energy to renewable energy sources.

B. INCREASED PUBLIC INTEREST IN RENEWABLE ENERGY

Energy is an integral component of the global economic growth engine. According to the report by International Energy Agency (IEA) in 2017, against the backdrop of a robust global economic growth of 3.7%, the global energy demand peaked at an estimated 14,050 million tonnes of oil equivalent (Mtoe). This was significantly higher than the global energy demand of 10,035 Mtoe in 2000 [9]. Another key take-away from the report was that throughout the period of global economic growth from 2000 to 2017, the overall share of fossil fuels remained at approximately 81% [9]. This suggests that despite improvements in global energy efficiency and growth in renewable energy sources and technologies, fossil fuels remain as the main energy source. It also meant that there had been equivalent increases in the use of fossil fuels to generate electricity, to power automobiles and to power industrial processes.

Correspondingly, with the rise in global energy demand, global carbon dioxide (CO_2) emissions reached a historic high of 32.5 giga-tonnes (Gt), as shown in Figure 1. These figures have huge implications as CO_2 emissions from the combustion of fossil fuels for energy production alone, contribute to 70% of the global greenhouse emissions [9]. This rise in the level of energy-related CO2 emissions would equate to a similar rise in the overall level of greenhouse gases.
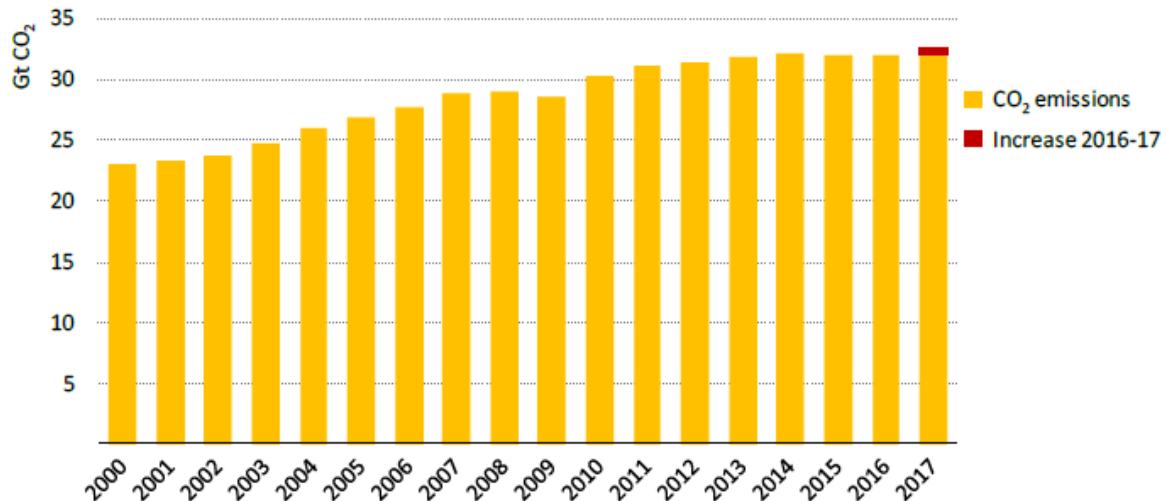
Figure 3.   Global Energy-Related CO_2 emissions, 2000–2017. Source: [9].

This was a major setback to the global efforts in tackling global warming. Since the turn of the century, there had been a rise in general awareness of the detrimental side-effects of combustion of fossil fuels for energy production such as the rise in the average global surface temperature. The issue of global warming poses a key dilemma for governments around the world as they struggle to find a balance between maintaining a sustainable economic growth and limiting the effects of global warming attributed by the CO_2 emissions from the usage and combustion of fossil fuels.

At the 2015 Paris Climate Agreement, G20 nations pledged to reduce their carbon budget to limit the global warming to below $2^{\circ}C$ by reducing global CO_2 emissions by 45.0% (13.5 Gt) from the 2017 CO_2 emission levels by 2030 and achieve net zero global CO_2 emissions by 2050 [10]. This was a significant moment in the global efforts in tackling global warming as the G20 nations represent 85% of the world economic output and contribute to 77% of the global greenhouse emissions [11]. To achieve these targets of reducing global CO_2 emissions, the key direction adopted by the G20 nations is to reduce the reliance on fossil fuels for energy generation by utilising renewable energy sources and technologies on a greater scale. This emphasis was re-iterated in the recent United Nations Emission Gap Report 2017, which served as a milestone report for the commitments pledged by the G20 nations. In this report, there was a Mission 2020's six-point plan which laid out the need for greater utilisation of renewable energy sources for all the key sectors such as electrical generation, building and infrastructures, transportation and industry. The plan also proposed for massive injects of

funds, up to $1 trillion USD annually, to scale up the existing renewable energy solutions rapidly [11]:

1.   To increase the electricity generation by renewable energy sources from 23.7% (6392 TWh) to 30.0% (approximately 7700 TWh) by 2020.

2.   To fully de-carbonise buildings and infrastructure by 2050.

3.   To halve emissions of heavy industries by 2050.

C.   INCREASED PUBLIC INTEREST DRIVING EXPONENTIAL GROWTH OF RENEWABLE ENERGY PROJECTS

In 2017, global renewable energy projects grew at an unprecedented year-on-year rate of 23%. Figure 4 shows that, at the end of 2017, the key renewable energy sources such as hydro energy, solar energy, wind energy and geothermal power contributed to a total global renewable capacity of 2,196 GW [8, 9] and accounted for a quarter of the global electricity generation at 6393 TWh [12].
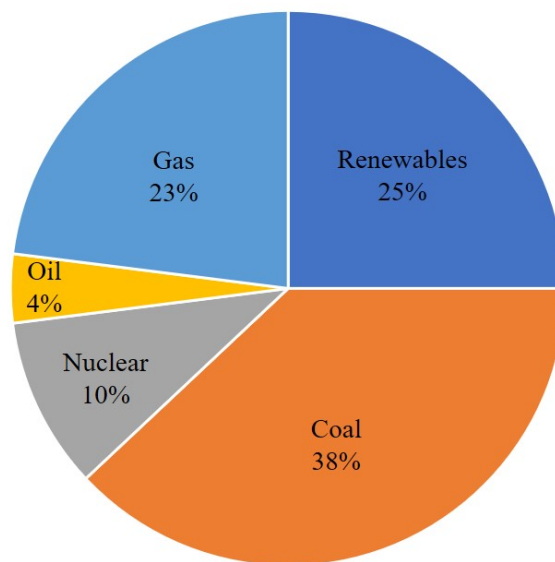
Figure 4.   Global Electricity Generation 2017. Source: [9].

For the United States, renewable energy sources currently account for approximately 17% of the total electricity generation at 0.68 trillion kWh [12]. The Renewable Electricity Futures Study that was commissioned by the Department of Energy's National Renewable

Energy Laboratory (NREL), projected that with increasing investments in renewable energy projects and improvements to the electrical systems, the United States would be able to generate up to 80% of her electricity generation from renewable energy sources by 2050 [13].

Figure 5 shows the general trend of lowering cost for renewable technologies. Cost of renewable technologies would continue to lower and coupled with the expectations that renewables would need to grow at a substantial rate to meet the Paris Agreement net zero CO_2 emission targets, the stage would be set for an exponential growth of renewable energy sources leading up to 2050. To provide a better sense of the scale of expected growth, a study done by a German-based energy watch group suggested that the globally installed renewable generating capacity could grow by one-fold from 2,196 GW to 4,450GW by 2030 [14].
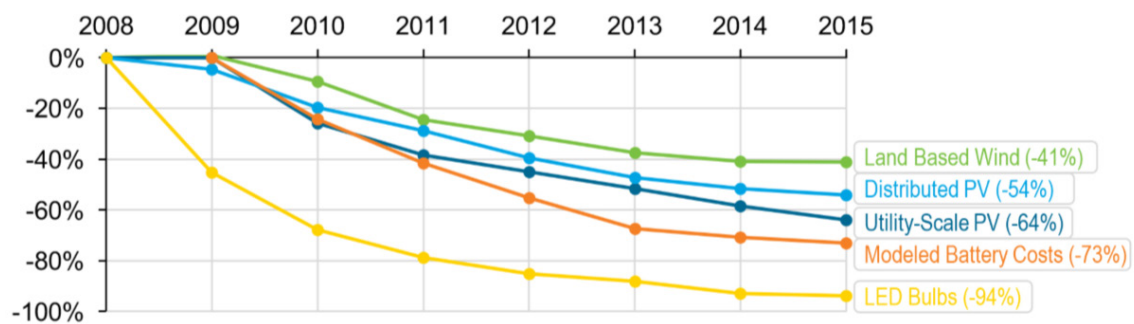
Figure 5.   Cost Reduction of Renewable Energies Since 2008. Source: [15].

D.   ELECTRICAL ENERGY STORAGE SOLUTIONS TO COUNTER INTERMITTENCY OF RENEWABLES

While renewable energy sources are positioned as the perfect alternative to fossil fuels for electrical power generation, there are challenges in the ability to harness and utilise the renewables as a stable and reliable form of energy [2]. Renewable energy sources tend to be intermittent by nature and the electrical power supply generated from these renewable sources would fluctuate with the ambient conditions. The fluctuations in power supply would pose serious stability and reliability issues to the electrical power grid.

To illustrate, in the case of harnessing solar energy with the solar photovoltaic (PV) panels, power generation would only occur during periods of daylight. As for harnessing wind energy, power generation could be highly irregular due to the volatility of wind power. This intermittent power generation could be mitigated with electrical energy storage solutions so

that power generation during peak ambient conditions could be stored and reserved for usage during off-peak periods.

In gist, electrical energy storage would allow the de-coupling of energy generation from consumption. As shown in Figure 6, the energy storage could be used for load levelling of consumers' electrical energy demands. This would reduce the need to constantly monitor and predict consumer peak energy demands as well as reduce the need to build reserve energy production plants to manage average demands rather than peak demands [16].
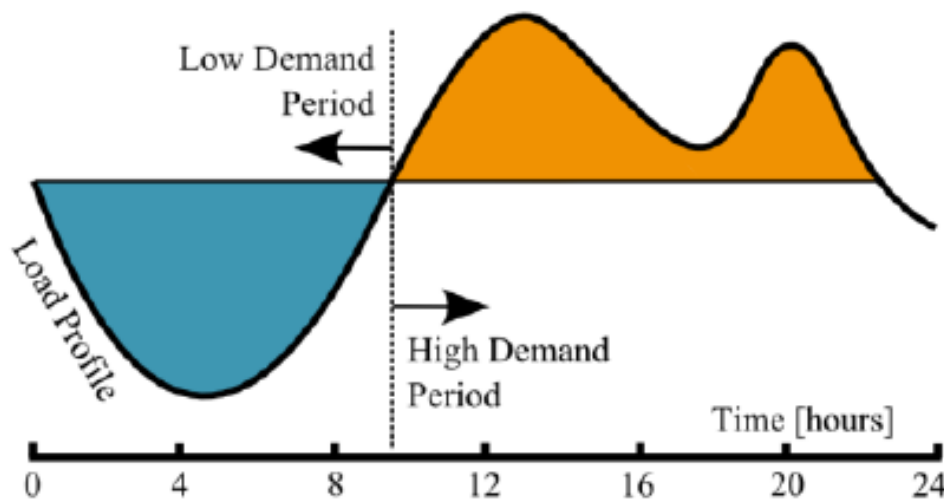
Figure 6.   Consumers Electrical Energy Demands with Load Levelling.
Source: [16].

With the renewable power generation market expected to grow exponentially leading up to 2050, the energy storage solutions would also need to grow in tandem to ensure continuous availability of these clean renewable power. The Bloomberg New Energy Finance projected that, in the lead up to 2030, an estimated $103 billion would be invested into the global energy storage market. The global energy storage could increase twelve-fold and expand to more than 300 GWh and 125 GW of capacity by 2030 [17].

E. TYPES OF ELECTRICAL ENERGY STORAGE

Electrical Energy Storage refers to the process of converting electrical energy into a stored form which can be re-converted back into electrical energy when required [18]. Table 1 shows the different technologies for electrical energy storage.

Specific to the compressed air grid storage, geographical limitation was highlighted as a disadvantage of the technology. Traditionally, the commercial large-scale CAES would require large underground storage caverns for compressed air storage. However, this limitation would not be valid for building-scale type of CAES whereby compressed air could be stored in storage tanks and easily integrated to buildings for consumer usage.

Table 1.   Summary of Grid Storage Technologies Comparison Metrics. Source: [18].

Metric	Hydro	Flywheel	Lead-acid	NMH	Thermal	Li	Advanced Li	Flow	Liquid Metal	Compressed Air
Specific Energy (kW/ kg)	.3-1.33	5-200	30-50	30-90	10-250	90-250	unknown	10-90	100-240	3.2-60
Energy Density (kWh/ volume)	.5-1.33	.25-424	25-90	38.9-300	25-370	94-500	unknown	5.17-70	150-345	.4-20
Specific Power (W/ kg)	.001-.12	400-30,000	25-415	50-1,000	10-30.0	8-2,000	unknown	5.5-166	14.29-260	2.2-24
Cycle Life	20-50k	Indefinite	200-2,000	300-10,000	Indefinite	500-10,000	2,000-5,000	10,000+	5,000-10,000+	5,000-20,000+
Useful Life	50-60	20	10-15	5-10	20+	5-15	unknown	5-20	10	25-40
Lifecycle Comments	Near universal life with maintenance	Near universal life with maintenance	Useful life varies with depth of discharge and application, variations by chemistry	Allows deeper depth of discharge and more stable storage, variations by chemistry	Thermal salts not yet proven, passive storage varies by technology	Useful life varies with depth of discharge and application, variations by chemistry	New chemistries not fully proven	Moving parts require replacement intermittently	Not yet proven	Near universal life with maintenance
Cost per kWh	$1-291	$200-150,000	$50-1,100	$100-1,000	$1-137	$200-4,000	unknown	$100-2,000	$150-900	$1-140
Environmental Impact	High/ Mixed	Low	High	High/ Med	Low	High/ Med	High/ Med	Medium	Low	Low/ Med
Pros	Large power capacity, positive externalities	Very fast response, high specific power, low cost, long life	Mature tehnology with established value proposition	Deep discharge capacity, reliable, high energy density	Could pair with waste heat generation, scalable, low cost, large scale	Flexible uses, very fast response and high specific power	Unknown comparisons to standard Li	Large storage capacity, cheap materials	High capacity, fast response, cheap materials, highly stable, temperature tolerant	Low cost, large scale, mature technology paired with gas turbines
Cons	Geographically limited, expensive construction, low energy density and environmentally damaging	Low energy density	Low lifecycle, toxic materials, flammability risks	Some toxic variations, less specific power than Li, high self-discharge, high memory effect	Not fully commercialized or not electrified	Safety concerns, low depth of discharge, corrosion, self-discharge and efficiency loss over time	Unknown comparisons to standard Li	Space requirements, economic efficiency in multiple applications	Untested in commercial use, persistent technology issues	Geographically limited

Currently, in the United States, pumped hydroelectric storage (PHS) is the dominant form of electrical energy storage and accounts for 94% (23.6 GW) of the U.S. deployed form of electrical energy storage. This is followed by three other major electrical energy storage systems: Compressed Air Energy Storage (CAES) at 114 MW, Advanced Battery Energy Storage (ABES) at 750 MW and Flywheel Energy Storage (FES) at 58MW [4]. The working principles of the four major electrical energy storage systems will be discussed in detail.

For PHS, the electricity generated during off-peak periods, is used to pump the water from a lower reservoir to a higher reservoir, as shown in Figure 7. During peak hours, electricity is generated by releasing the water in the higher reservoir to flow through and turn the turbine. PHS has a long lifetime, typically 50–60 years, and provides large storage capacity with a high cycle efficiency of at least 75% [4]. In addition, the PHS technology is relatively mature and can be readily deployed. However, further utilisation of PHS is limited by geographical constraints, high capital and costs and possible adverse impacts to the environment.
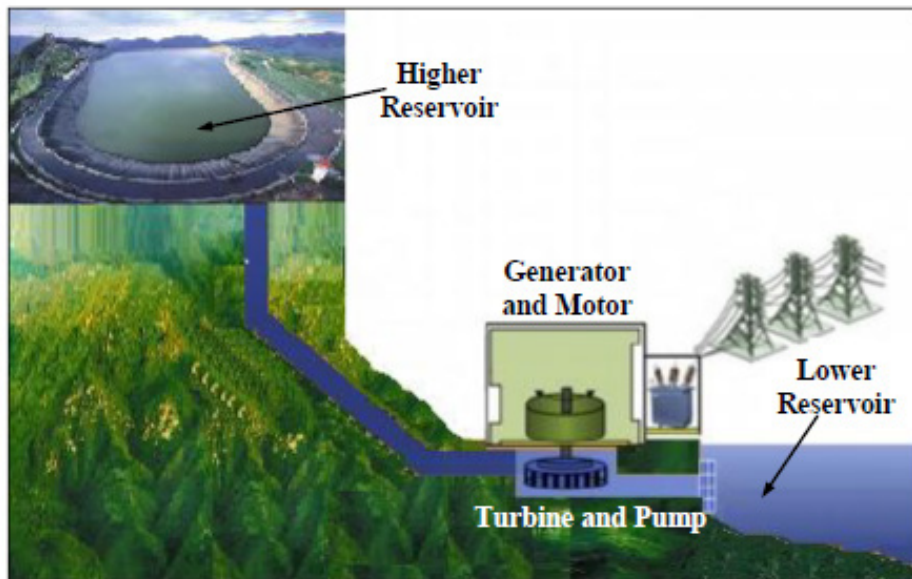
Figure 7.   Pumped Hydroelectric Storage. Source: [19].

ABES refers to energy storage projects that utilise lithium-ion, lead-acid, nickel-based, sodium-based and flow-based batteries. During off-peak periods, the energy is stored in the form of chemical energy by using electricity to charge the batteries. During peak periods, the stored energy is released directly back to the electrical grid to meet the increased electrical demands. Plants operating on ABES typically have efficiencies of 60–95% [4].

For FES, a rotor is spun in a practically frictionless enclosure and the electric energy generated is stored in the form of kinetic energy. To meet and level the different loads throughout the day, the rotor is either sped up or down to transfer energy between the FES and the electrical grid. Plants operating on FES typically have efficiencies of 85–87% [4].

For CAES, energy is stored in the form of high pressure compressed air which is then stored in underground caverns, as shown in Figure 8. During off-peak periods, electricity is used to compress air to high pressure using air compressors. During peak periods, the stored compressed air is released through expanders to generate electricity to meet the increased demands [4].
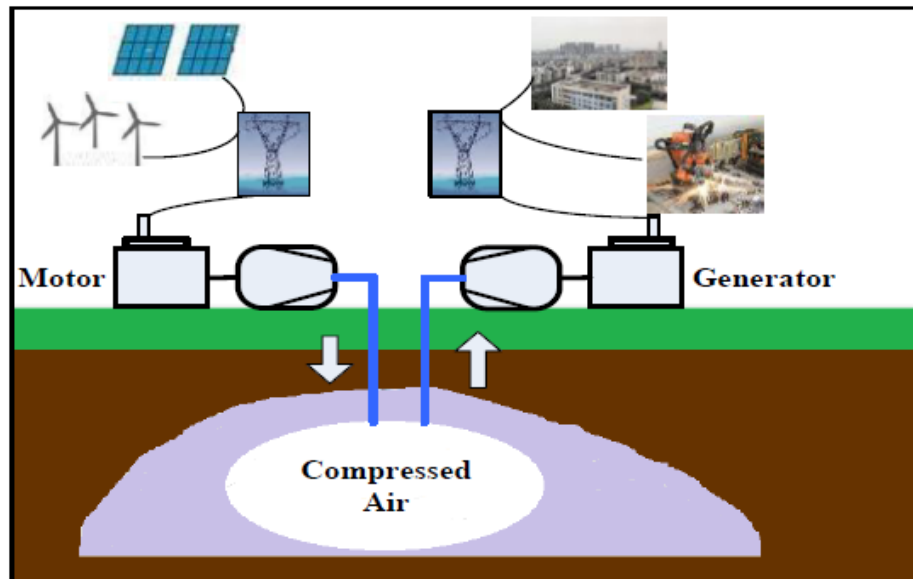
Figure 8.   Compressed Air Energy Storage. Source: [19].

F. WHY THE FOCUS ON CAES?

CAES is the only other commercial large capacity storage alternative to PHS. Compared to PHS, CAES results in lesser environmental impact and possesses higher volumetric and power outputs. The other key point is that CAES can be used for long or short duration storage at many scales at low capital cost [19]. This scalability feature at low economic cost gives CAES the potential to become the dominant form of electrical energy storage across the entire spectrum of electrical grid applications.

The rest of the literature review will focus on the technology development and future trend of CAES, with a specific lens on small-scale utility CAES systems, for integration to buildings. Unlike commercial large-scale CAES, small-scale utility CAES systems would not be limited by the geographical constraints of requiring large underground storage caverns. This would mean that small-scale utility CAES technology could be easily integrated to buildings and military installations for end user usage.

G. TYPES OF CAES

CAES system is typically made up of primary components such as the gas turbine, compressor and combustor. CAES is based on the working principle of gas turbine plant, where the working medium which consists of air and gas, undergo two different stages of expansion and compression operations. A mixture of compressed air and fuel, at high temperature and pressure, is fed into the turbine to drive the generator to generate electricity [19].

Figure 9 shows the four types of commercial CAES configuration: Diabatic (D-CAES), Adiabatic (A-CAES), Advanced adiabatic (AA-CAES), and Isothermal (I-CAES). One of the key differences is that the D-CAES system stores compressed air in geological underground caverns while the other three systems store compressed air in CAES storage tanks. The other key difference between the 4 major systems lies in the management of the excess heat produced by the air compression process [20].
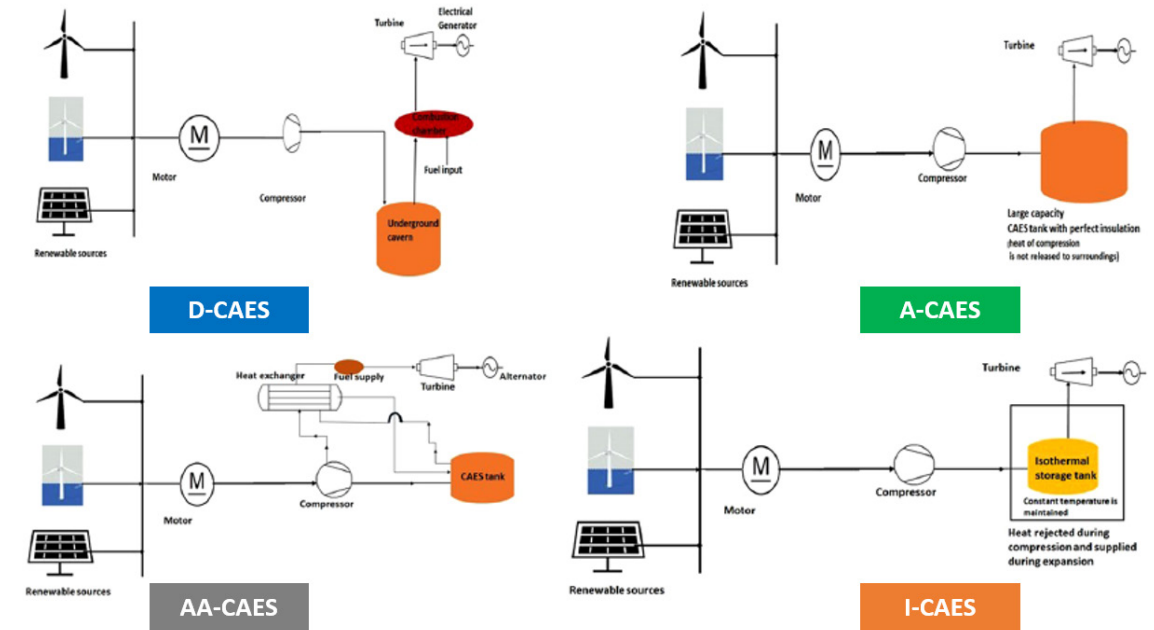
Figure 9.   Four Major CAES Configurations. Source: [20].

For D-CAES system, the heat from the compression of air is dissipated as waste heat. The system requires the combustion of fossil fuel (natural gas) to heat up the compressed air before the expansion process [20].

For A-CAES system, the air is heated up during the compression process and the higher temperature air is stored within the adiabatic storage tanks. While the power generation output from a higher temperature gas is expected to be higher, the system would require a larger volume of storage tanks to hold more mass of air at a higher temperature [20].

For AA-CAES system, the heat generated from the compression process is recovered and stored in a separate thermal storage medium. During the expansion phase, the heat energy stored in the thermal storage medium is utilised for heating the compressed air [20].

For I-CAES system, the temperature of the compressed air storage tank is maintained at a constant temperature. The constant temperature of the tank is achieved by

the removal of heat during the charging process and resupply of heat during the discharging process [20].

H.   OPERATING UTILITY-SCALE CAES

Presently, the two largest utility scale CAES plants have a combined capacity of 430MW. One plant is in Huntorf, Germany (320 MW), shown in Figure 10. The other plant is in Macintosh, Alabama (110 MW) in the United States [21]. There are 3 other smaller operating CAES plants in the United States of about 4 MW with efficiencies of 42–55% [4].

Currently, all these commercial CAES plants are D-CAES systems and there are two significant drawbacks. Firstly, these CAES plants do not necessarily provide 'clean' energy as the D-CAES process require the combustion of natural gas to heat up the gas before the expansion process. This would result in CO_2 emissions. Secondly, there are geographical constraints in locating underground caverns that can store large mass of compressed air.
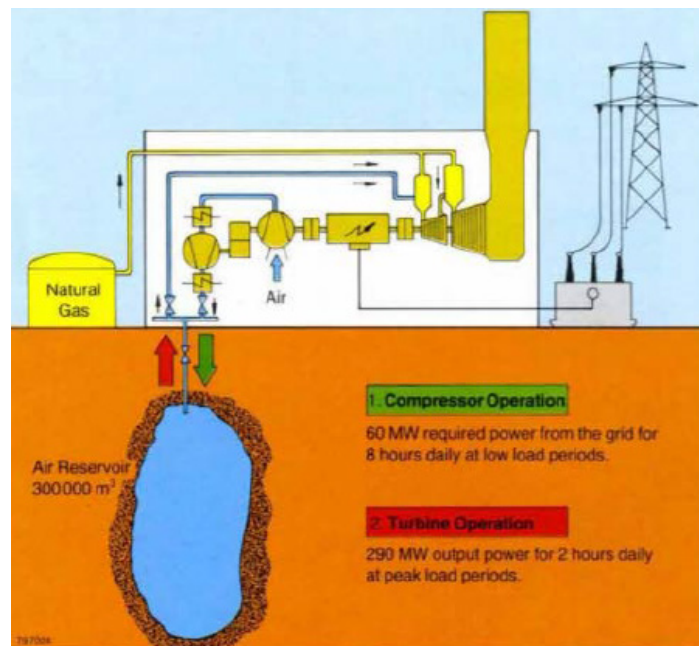
Figure 10.   Structure of Huntorf CAES Plant in Germany. Source: [22].

I. UTILITY-SCALE CAES IN DEVELOPMENT

The biggest German electric utilities company RWE launched the first AA-CAES plant, Project *ADELE* (Advanced **AD**iabatic compressed-air storage project for **ELE**ctricity supply). Project *ADELE* is designed to be a 260MW plant with a projected efficiency of up to 70% [23]. The most important characteristics is that the plant will have zero CO_2 emission as there is no requirement for the combustion of fossil fuels. The heat released from the compression of air is captured in the thermal energy storage facility and the heat energy is released into the compressed air during the expansion process. Figure 11 shows an artist's impression of the design of Project *ADELE*.
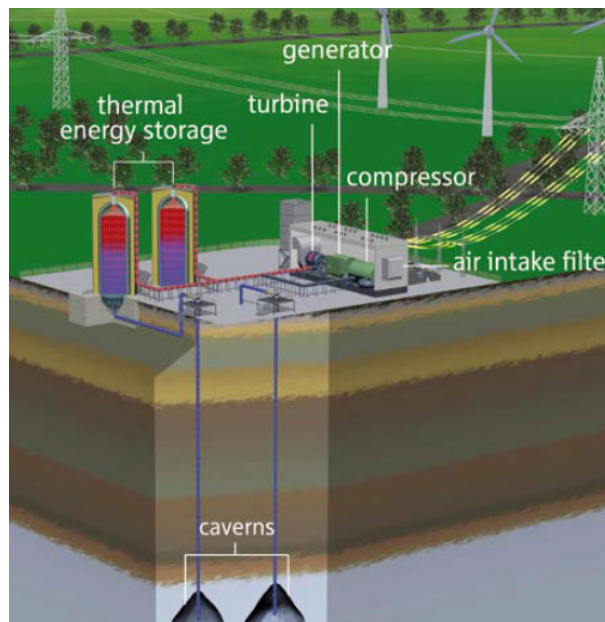
Figure 11.   Artist's Impression of Project *ADELE*. Source: [23].

As shown in Figure 12, a Canadian start-up Hydrostor started a pilot 1MW project to create the world's first novel offshore compressed air energy storage in Lake Ontario, Toronto-Canada [24]. The compression of air is done by the land-based compressors and the waste heat is captured by thermal storage facilities to reheat the compressed air during the expansion process. The compressed air is pumped and stored in the balloons which are located on the ocean floor. When electricity is needed, the system reverses the process and

the weight of water would push the air back to the air turbines on land, to generate electricity. Hydrostor projected the capital and storage cost of compressed air in offshore facilities to be $250 per kW, which would be significantly lower than the capital and storage cost of $400–$800 per kW for underground caverns storage [25].
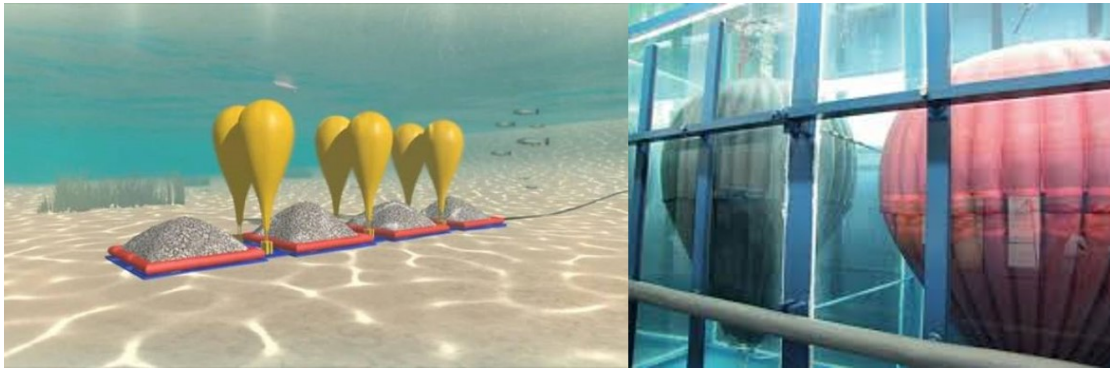
Figure 12.   Offshore Compressed Air Energy Storage Project. Source:
[24].

As shown in Figure 13, a pilot plant operating under the concept of Liquid Air Energy Storage (LAES) was built and transferred to the University of Birmingham. Figure 14 shows the schematic diagram of the LAES system. At the charging phase, the air would be liquefied and stored in a tank at low temperature. At the discharging phase, the liquefied air would be expanded and heated in the expanders to drive motors. Theoretically, the LAES system has an energy storage density of 73% and a cycle efficiency up to 80% [19].
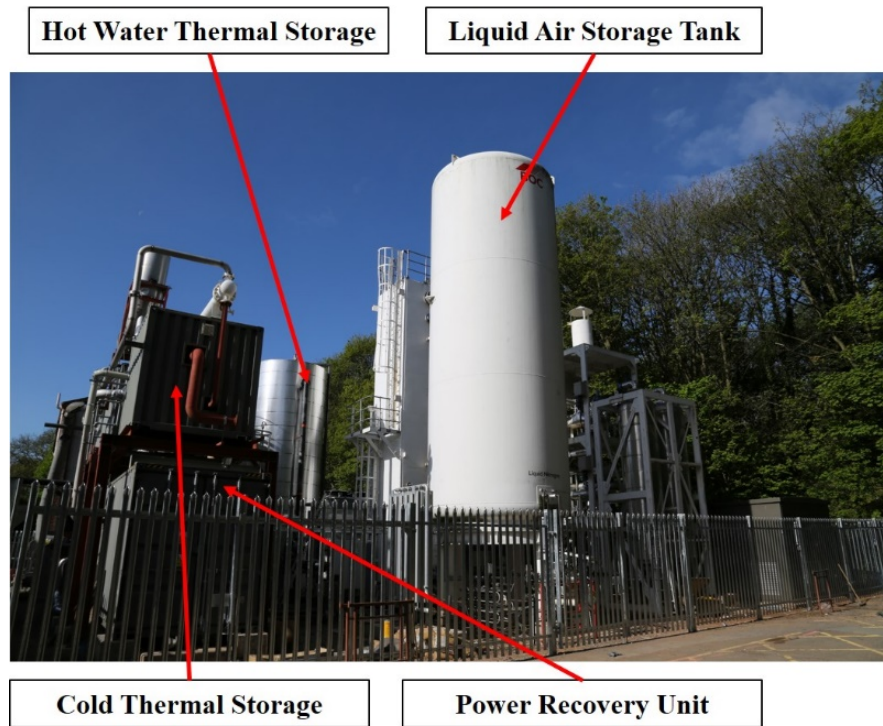
Figure 13.   350 kW/ 2.5 MWh LAES Pilot Plant at Birmingham. Source: [26].
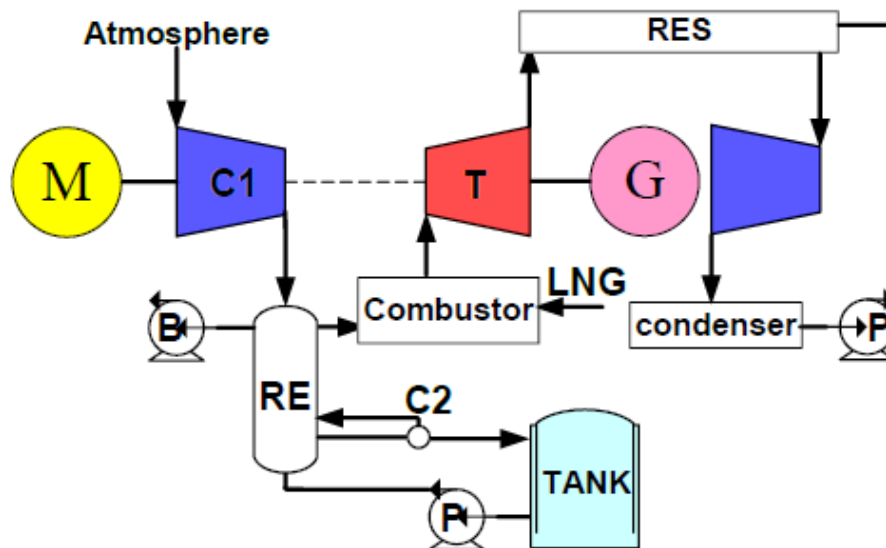
Figure 14.   Schematic Diagram of LAES System. Source: [19].

As shown in Figure 15, a 1.5 MW Supercritical Compressed Air Energy Storage (SC-CAES) pilot project had been under demonstration in Beijing and successfully operated for 3000 hours with a system efficiency of approximately 55% [19]. Figure 16 provides a schematic diagram of the SC-CAES system. Theoretically, the SC-CAES system is a novel CAES system which stores the compressed air in supercritical state and possesses advantages such as high energy density (18 times higher than conventional CAES) and high thermal efficiency (up to 68%) [19].

Figure 15.   A 1.5 MW SC-CAES Plant in China. Source: [19].
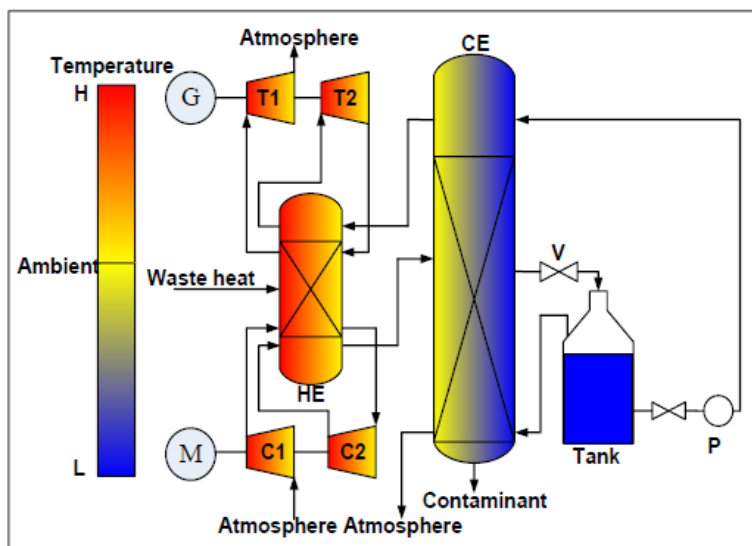
Figure 16.   Schematic Diagram of SC-CAES System. Source: [19].

J.   APPLICATIONS OF SMALL SCALE CAES (SS-CAES) TO MILITARY INSTALLATIONS

By broad definitions, small-scale CAES systems refer to systems of less than 10MW in capacity and store compressed air in man-made storage vessels instead of underground caverns. Table 2 provides a summary of the different categories of CAES. Since CAES could be scaled and integrated with renewable energy sources, there had been a growing interest in the technological area of small-scale CAES and renewable energy integration for commercial, residential and military buildings. However, there had been limited experimental performance data on the operation of small-scale CAES systems.

Table 2.   Categorization of Scales of Energy Storage. Adapted from [20].

Category	Power Rating	Possible Applications
Small Scale	< 10MW	Mobile Devices, Electric Vehicles, UPS of Office Buildings
Medium Scale	10 – 100 MW	Remote Communities and Towns
Large Scale	>100MW	Power Plants

In 2018, a team from the University of Perugia carried out a performance analysis by applying data from their experimental Solar PV integrated with SS-CAES prototype and a proposed thermodynamic model to a residential building, with floor area of 280m^2 in Citta di Castello in Central Italy. Their analysis showed that 26% of the energy demand of the building was met by a small CAES area outlay of 2.5m^3 with a storage volume of 0.25m^3 of 225 bar compressed air [27].

This study was the first-of-its kind and introduced experimental data of CAES prototype for residential building application. The study showcased and demonstrated the feasibility of installing a SS-CAES system integrated with renewable energy source in a residential building. Potentially, SS-CAES systems could significantly improve the energy resiliency aspect of military installations by fulfilling two key functions. Firstly, SS-CAES could be used as back-up power or uninterrupted power supply (UPS) in cases of power system failures, to supply power to key military installations, data processing centers and hospitals. Secondly, SS-CAES could offer power-grid independence of military installation by providing dark start capability in a complete power shutdown condition. Dark start would refer to the ability of the system to restore itself back to operation from an electrical blackout due to disruption in the external power supply [28]. For example, the Huntorf plant could provide dark start capability to nuclear plants located near North Sea during a complete power outage [19]. In another example, the compressed air reserves onboard U.S. Navy (USN) ships, would provide ships with the dark start capability to air start the gas turbines in the event of a blackout [29].

THIS PAGE INTENTIONALLY LEFT BLANK

III. SYSTEM ARCHITECTURE AND EQUIPMENT

A. OVERVIEW

The SS-CAES project at the Naval Postgraduate School Integrated Multi Physics Energy Lab (NPS IMPEL) is being developed under two separate but related tracks. The first track which involves the expansion phase, had been implemented and automated by McLaughlin and Vranas, respectively [5, 7]. The second track, which involves the compression phase, was analysed, implemented and automated by Prinsen and Williams, respectively [6, 8].

This thesis focuses on enhancements to the system architecture and programming logic to achieve a proof-of-concept of the full automation of the SS-CAES compression phase. Figure 17 provides an overview the current system architecture of the SS-CAES compression phase

B. SYSTEM ARCHITECTURE

Figure 17 is the system architecture of the compression phase of the SS-CAES. A short description of the operation of the SS-CAES compression phase is provided.
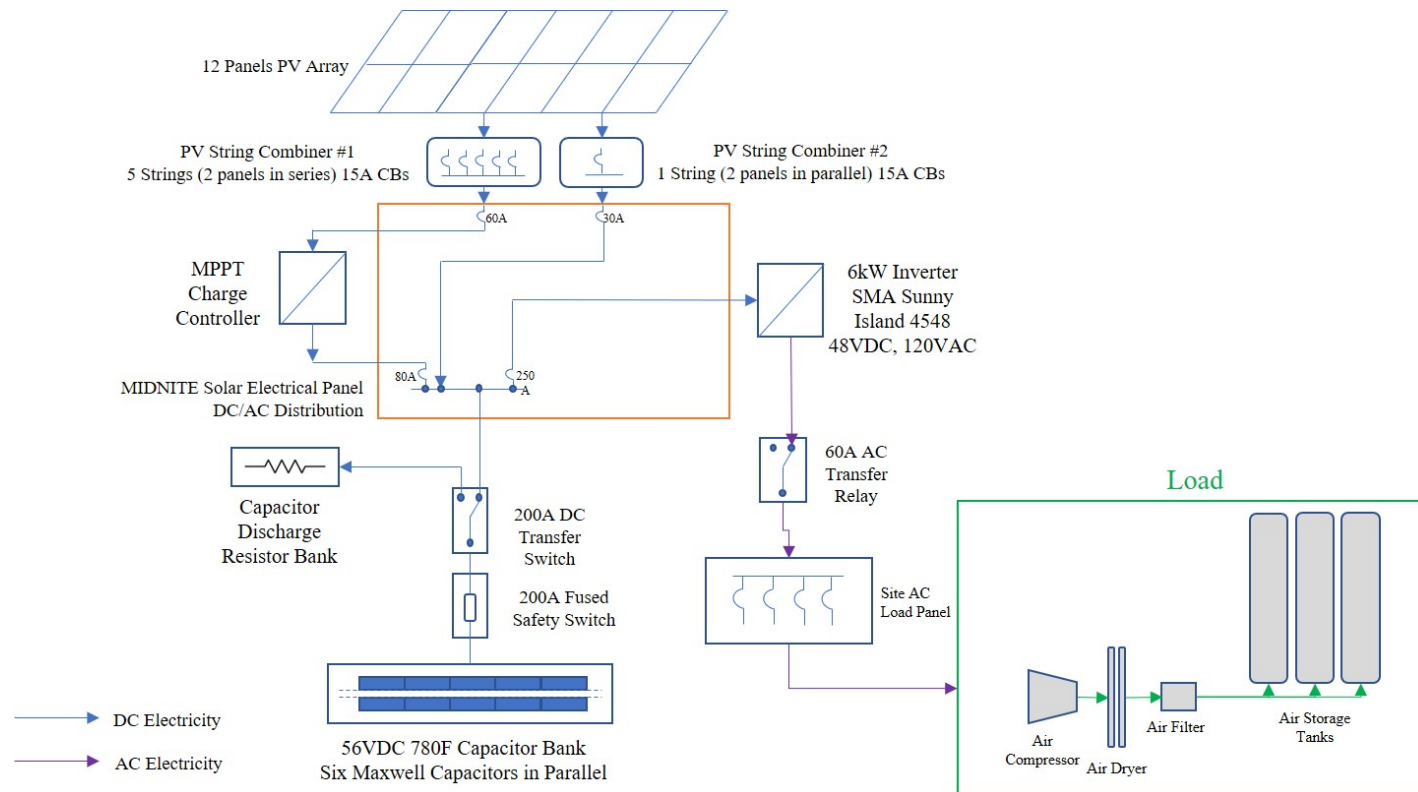

Figure 17.   System Architecture of SS-CAES Compression Phase.

The 12-panels Photovoltaic (PV) array is responsible for electricity production by converting solar radiance to electrical energy. One string of 2 solar panels is dedicated to charge the Capacitor bank to the required voltage to provide startup power to the charge controller. When the charge controller is in operation, it would run the Maximum Power Point Tracking (MPPT) algorithm to continuously sample and maximise the voltage and current output of the PV arrays. The charge controller provides the required output to power the inverter and charge the capacitor bank with the excess output from the PV array. The inverter converts the electrical current from Direct Current (DC) to Alternating Current (AC), to power the air compressor and air dryer.

A key feature of the SS-CAES would be the dark start capability that was designed and embedded in the system architecture. In the unlikely event that the PV array could not generate electricity due to poor solar irradiance and the capacitor bank was completely drained, the compressed air reserves from the storage tanks could be released to air start the air-driven generator. The electricity produced by the generator would be able to power the MPPT, inverter and recharge the capacitor bank rapidly.

C.   EQUIPMENT

As the thesis focuses on improving the electrical aspects of the system architecture and the logic of the automation program, this section would provide descriptions of the SS-CAES components that are involved in the capture, conversion and transfer of digital signals and electrical energy only. The components of interest are: (1) PV array, (2) MidNite Classic 150 MPPT charge controller, (3) Maxwell Supercapacitor bank, (4) SMA Sunny Island DC to AC inverter, (5) Allen-Bradley Micro850 Programmable Logic Controller (PLC) and (6) BK Precision power supply module. Details of the mechanical components of the SS-CAES compression phase can be found in the thesis work of Williams [8].

1.   Photovoltaic Array (Solar Panels)

The PV array covers a total area of $19.3m^3$ and generates a maximum power of 3.36kW. The 12 panels are arranged into 6 parallel strands. The first strand with two panels

connected in parallel, generates a maximum of 36 volts direct current (VDC) for the pre-charging of the capacitor bank. The other five strands, each with two panels connected in series, generate a maximum of 79 VDC [6]. Figure 18 shows the PV array installed in the NPS IMPEL for the SS-CAES.
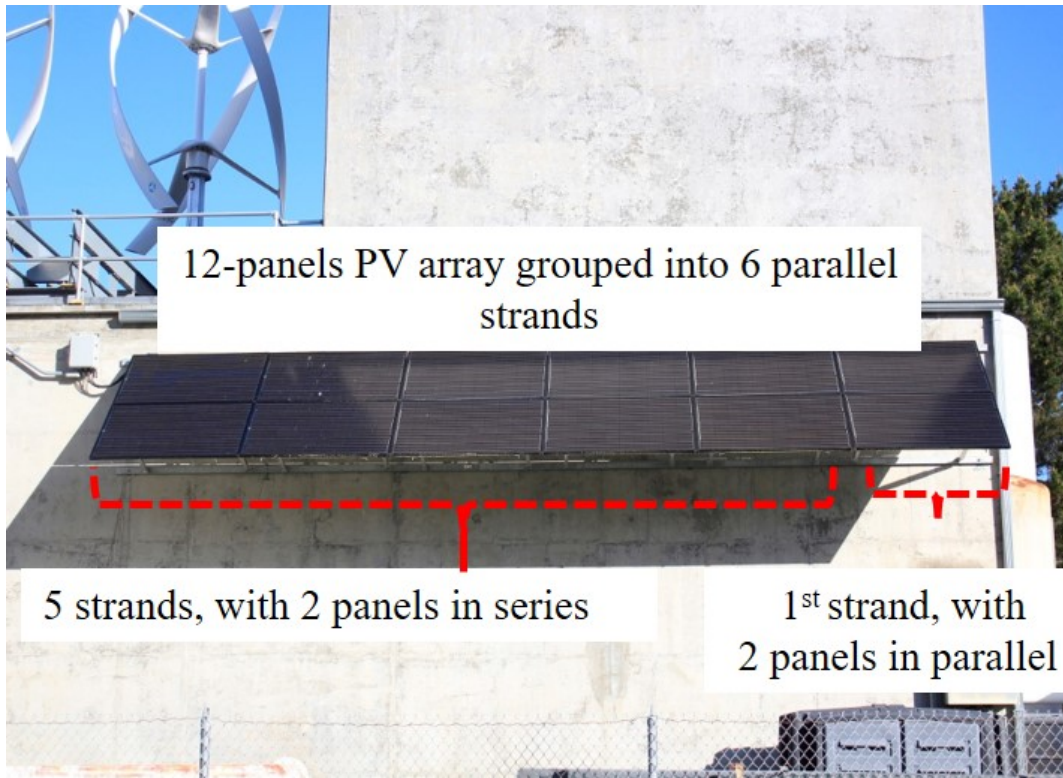
Figure 18.   SS-CAES Solar Panel Array at NPS IMPEL

2.   MidNite Classic 150 MPPT Charge Controller

The solar charge controller installed for the SS-CAES is the MidNite Classic 150 charge controller. The charge controller in Figure 19, is embedded with MPPT algorithm which would ensure that the PV array operates at the most efficient voltage, also known as maximum power point and allow the charge controller to extract the maximum available power from the PV array [8]. In terms of working principles, the controller embedded with the MPPT algorithm would continuously scan and sample the available output voltage of the PV array. The controller would then determine the optimal voltage and current that the

PV array should produce to charge the storage medium by comparing the output voltage of the PV array and the voltage of the storage medium [30]. Therefore, the utilization of a MPPT charge controller would ensure maximum power available to the storage medium and increase the efficiency of the entire microgrid. In addition, another key feature of the charge controller was its ability to support Modbus Protocol for interface communication with the PLC for automation of the compression phase [31].

Figure 19. MidNite Classic 150 Charge Controller and Electrical Panel. Source: [31].

3.   Maxwell Supercapacitor Bank

The supercapacitor was selected as the temporary energy storage medium for the microgrid. Due to the supercapacitor's ability to undergo rapid charge and discharge cycles, the supercapacitor would be most suited to perform load-levelling functions in building microgrids. In addition, the supercapacitor possesses high power and energy density and relatively long service life of 10 to 15 years [32]. Specific to the SS-CAES, a total of 6 sets of Maxwell BMOD0130 P056 B03 ultracapacitors were installed and

arranged in parallel [8]. As shown in Figure 20, each supercapacitor set is rated at 56 VDC and 130 farads [33]. Based on Equation (1), the 6 sets of supercapacitors arranged in parallel would provide a maximum capacitance of 780 farads.

$$C_{parallel,total} = C_1 + C_2 + C_3 + C_4 + C_5 + C_6 \qquad (1)$$

Based on Equation (2), the expected total energy stored in the capacitors is calculated to be 339.7 Wh.

$$E_{stored} = \frac{\frac{1}{2}CV^2}{3600} \qquad (2)$$

However, based on previous bench testing conducted by Williams, it was found that the supercapacitors can only be charged up to 54.5 VDC [8]. This could be an inherent product design to prevent the capacitors from exceeding the breakdown voltage and inadvertently damaging the dielectric. This would result in a reduction of the total stored energy in the capacitor by approximately 5.2% to 321.8 Wh.

Rated: 56 VDC, 130F

Figure 20.   Maxwell BMOD0130 P056 B03 Ultracapacitor. Source: [33].

4. DC to AC Inverter

The inverter system installed for the SS-CAES is the SMA Sunny Island 4585-US-10 inverter, as shown in Figure 21. The inverter converts the incoming VDC supply from the charge controller and storage medium to 120 volts alternating current (VAC) supply. The 120 VAC supply would then be fed into the SMA SI-TD-BOX-10 Smartformer, to be transformed to the 240 VAC supply required for the operation of the air compressor.

Regarding the operation of the Sunny Island inverter, there were several pertinent issues highlighted by Williams. The inverter would not operate at voltages below 30 VDC, and it would enter self-protection mode and power off when the voltage fell below 25 VDC. This situation would typically occur after sunset when there was no electricity production by the PV arrays. For the inverter to remain in active operation, it would need to draw power from the ultracapacitor bank, and this would result in the draining of the capacitor bank to levels below 30 VDC before daybreak. Once powered down, the automation of the compression phase would cease, and the inverter would require a physical reset of at least 15 minutes before it could be restarted [8].

Figure 21.   SMA Sunny Island 4548-US-10 Inverter. Source: [34].

5.   Allen Bradley Micro850 Programmable Logic Controller

For the automation of the SS-CAES, there had been comparisons done between a PLC-based controller and a PC-based controller. In general, a PLC-based controller had clear advantages over PC-based controller in terms of reliability, practicability and cost [35]. To highlight, a key advantage of the PLC-based controller over the PC-based controller was the ability to preserve data during a power failure. For PC-based controller, a power failure incident could lead to major data corruption and potentially render the system inoperative.

As shown in Figure 22, the specific PLC-based controller chosen was the Allen-Bradley Micro850 Programmable Logic Controller (PLC). The Micro850 was chosen due to several key features that it offered. Firstly, infrastructure setup involving a Micro850 PLC would be relatively compact. This is because the Micro850 has 14 embedded digital input ports and 10 embedded digital output ports. Secondly, in terms of upgradability, the functions of the Micro850 could be easily increased through installation of additional analog modules on the plug-in latches or additional digital Input/ Output (IO) modules on the expansion ports. For example, if the project required the reading or writing of analog signals between the PLC and other devices, analog modules could be directly installed on the plug-in latches. Lastly, the Micro850 PLC could be easily programmed by the Connected Component Workbench software offered by the Rockwell Automation, which is the parent company of the Allen-Bradley brand [36].
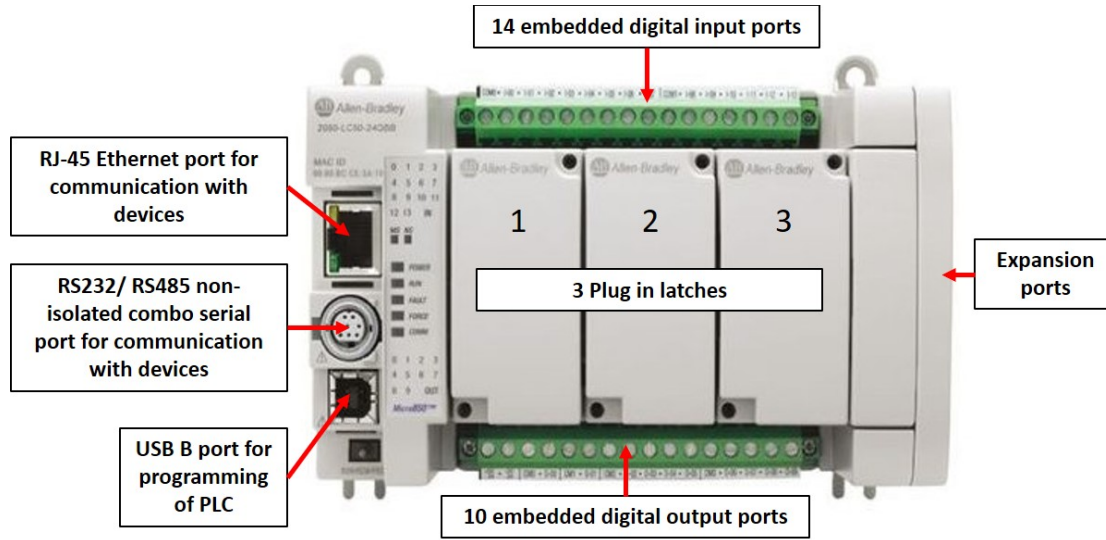
Figure 22.　Allen-Bradley Micro850 PLC. Source [36].

6.　Power Supply Module

The limitations to the automation of the SS-CAES due to the inverter going into standby at 30 VDC and eventually powering down at 25 VDC after sunset, had been discussed. While the integration of the expansion and compression phases of the SS-CAES is on-going, a proof-of-concept of the full-scale automation of the SS-CAES could be demonstrated with an interim solution of installing a power supply module to provide a power supply to the inverter and the capacitor bank after sunset. Once the compression and expansion phases are integrated, the power supply module could be the backup power supply to the air-driven generator.

There were several criteria that the power supply module needed to satisfy. Firstly, based on Table 3, the recorded data retrieved from the Modbus communication gateway showed that the inverter would draw at least 1.4A during normal operations. To provide system redundancy in terms of overall load amperage, the module should be able to supply an output current of at least 2.8A. Secondly, the module should be able to provide an output voltage of more than 30 VDC, to keep the inverter and charge controller powered on throughout the night. Thirdly, the module should have overvoltage protection feature so that it could be directly connected to the capacitor bank for charging. Lastly, the module should not be too costly to procure as it is meant to be an interim solution to demonstrate

the full automation capability of the SS-CAES. As shown in Figure 23, the power supply module selected is the compact benchtop 108W BK Precision Model 1550 Power Supply Module, which cost approximately $200 and could deliver a maximum output voltage of 36 VDC and current of 3A [37]. However, the power supply module could not support Modbus protocol and did not have inputs ports to read digital signals from the PLC. This could pose some limitations to the autonomous control of the module.

Table 3.   Recorded Data of Current Drawn by Inverter During Normal Operations

TimeStamp	Capacitor Voltage	Inverter Current	Inverter Status
hh:mm	V	A	
16:00	53.37	1.27	3: Run
16:15	53.37	1.4	3: Run
16:30	53.37	1.4	3: Run
16:45	53.39	1.4	3: Run
17:00	53.4	1.4	3: Run
17:15	53.4	1.4	3: Run
17:30	53.4	1.4	3: Run
17:45	53.32	1.4	3: Run
18:00	52.83	1.4	3: Run
18:15	51.52	1.4	3: Run
18:30	50.18	1.4	3: Run
18:45	48.82	1.4	3: Run
19:00	47.5	1.4	3: Run
19:15	46.15	1.4	3: Run
19:30	44.78	1.4	3: Run
19:45	43.45	1.4	3: Run
20:00	42.15	1.4	3: Run
20:15	40.88	1.4	3: Run
20:30	39.59	1.4	3: Run
20:45	38.33	1.4	3: Run
21:00	37.05	1.4	3: Run
21:15	35.78	1.4	3: Run
21:30	34.49	1.4	3: Run
21:45	33.15	1.4	3: Run

Details of the hardware and software integration of the power supply module to the overall system architecture would be discussed in the later chapter on design, implementation and testing.

Figure 23.   BK Precision 1550 Power Supply Module. Source: [37].

THIS PAGE INTENTIONALLY LEFT BLANK

IV. DESIGN, IMPLEMENTATION AND TESTING

A. OVERVIEW OF DESIGN ISSUE

As highlighted in the earlier chapter, the current limitation to the automation process, would be the minimum voltage of 30 VDC required by the inverter for active operation. Based on the existing system architecture, the ability to sustain the minimum 30 VDC requirement for the inverter after sunset, was a key challenge. This was because, after sunset, the inverter and charge controller would draw its required power directly from the capacitor bank. Once the capacitor bank drained to a voltage level below 30 VDC, the inverter would immediately enter standby mode and the automation of the SS-CAES would cease. Table 4 shows a set of recorded data extracted from Modbus communication gateway. The data clearly showed that the inverter entered standby mode and completely shut down before midnight.

It is important to note that, with the integration and automation of the compression and expansion phases, this situation would not occur. Specifically, when the voltage of capacitor bank reached levels close to 30 VDC, the air-driven generator would be activated to produce electricity to directly power the inverter and re-charge the capacitor bank.

Therefore, to achieve a proof-of-concept of the full-scale autonomy of the SS-CAES, the interim solution would be to install a power supply to the system architecture and write a program to the PLC such that the power supply would assume the interim role of the air driven generator. The power supply module would power the inverter and recharge the capacitor bank, whenever the overall voltage of the capacitor bank drops below the 30 VDC after sunset.

B.   DESIGN CONSIDERATIONS

This section provides an overview of the design considerations in the integration of the hardware and software aspects of the power supply module to the SS-CAES system architecture.

1.   Hardware Design Considerations (Installation and Wiring)

Firstly, in terms of physical wiring, the power supply module would need to be connected to the common bus located inside the charge controller electrical panel. To prevent the power supply module from being damaged by backflow surge current from the bus towards the power supply module, a suppression diode would need to be installed between the module and the common bus.

Secondly, as discussed in the earlier chapter, there were some limitations in the autonomous control of the power supply module as it could not support Modbus protocol and could not read digital signals from the PLC. Therefore, to enable autonomous control of the module, a possible solution is shown in Figure 24. A circuitry could be designed for the power supply module to be activated by a solid-state relay (SSR) instead. In terms of working principle, the 24 VDC output signal from the PLC would energize the SSR and the power supply from the module to the common bus would be activated. An overview of the hardware integration of the power supply module to the system architecture is shown in Figure 25.
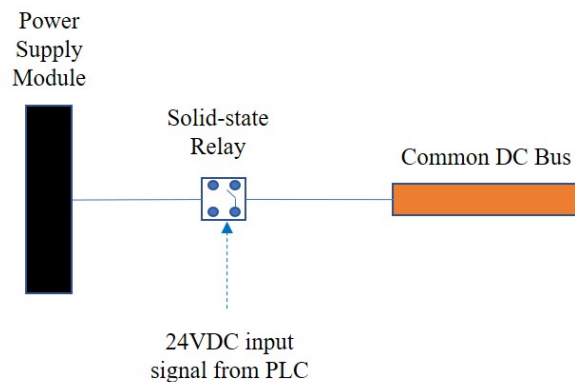
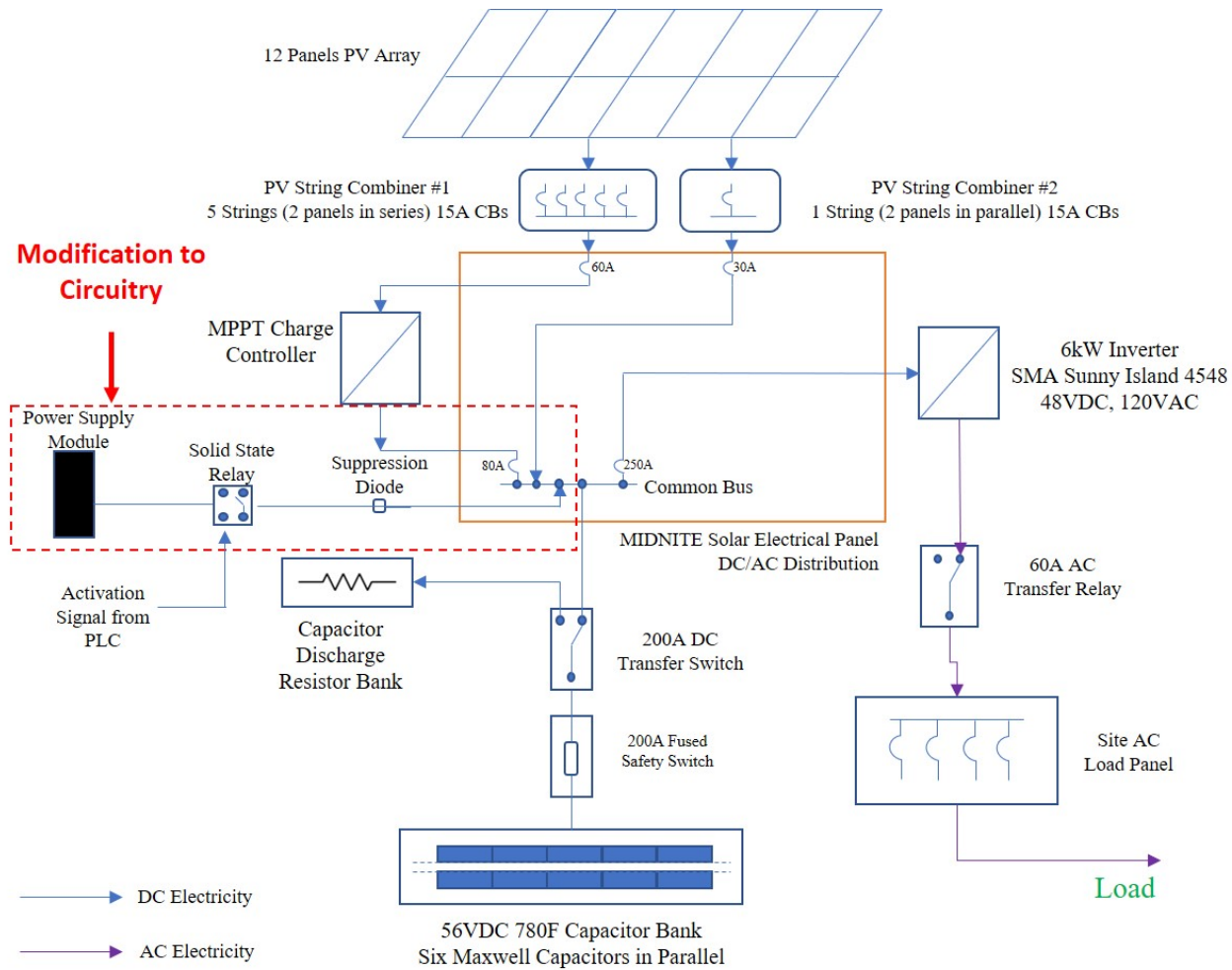Figure 24.   Control of Power Supply Module via SSR

12 Panels PV Array

PV String Combiner #1
5 Strings (2 panels in series) 15A CBs

PV String Combiner #2
1 String (2 panels in parallel) 15A CBs

Modification to Circuitry

60A

30A

MPPT Charge Controller

6kW Inverter
SMA Sunny Island 4548
48VDC, 120VAC

Power Supply Module

Solid State Relay

Suppression Diode

80A

250A

Common Bus

MIDNITE Solar Electrical Panel
DC/AC Distribution

60A AC Transfer Relay

Activation Signal from PLC

Capacitor Discharge Resistor Bank

200A DC Transfer Switch

Site AC Load Panel

200A Fused Safety Switch

DC Electricity

AC Electricity

56VDC 780F Capacitor Bank
Six Maxwell Capacitors in Parallel

Load

Figure 25.   System Architecture with Integration of Power Supply Module

37

2. Software Design Considerations (Programming the Control Logic)

In the design of the control logic, the first test would be to determine if the voltage of the capacitor bank was above 33 VDC. According to Williams, it was determined that the capacitor bank would need to be charged to a voltage of at least 33 VDC to sustain concurrent operations of the powering the inverter, charging the Capacitor bank and charge controller [8].

The second test would be to determine if the voltage of the capacitor bank was above 36 VDC. This was to ensure that the power supply module did not operate beyond its safe working range and disconnected from the common bus when the capacitor bank was charged to 36 VDC.

Therefore, when the PLC retrieved the voltage inputs of the capacitor bank from the MPPT charge controller via the Modbus gateway and determined that both tests did not meet the requirements, the SSR would be energised to activate the power supply from the module to the bus. Figure 26 provides an overview of the control logic to enable the supply of power from the power supply module to the common bus.
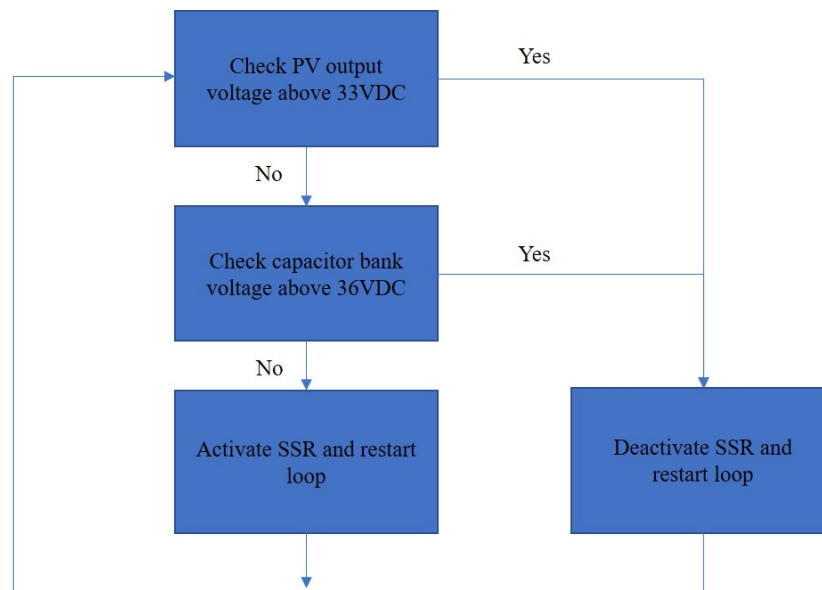

Figure 26.   Simplified Control Logic for Activation of Supply from
Power Supply Module to Common Bus

C. IMPLEMENTATION AND TESTING

The implementation and testing of the integration of the circuitry and program codes were broken into a few phases. Firstly, to determine the feasibility of controlling the activation of power supply from the power supply module to the common bus via the SSR, the circuitry was setup and bench tested. Next, a function block diagram (FBD) program to activate the power supply was written and integrated with the existing codes programmed by Williams. The new program was compiled and downloaded into the SS-CAES PLC. A quick verification test was done by observing if the embedded digital output port assigned to energize the relay was activated when the minimum voltage requirements of the capacitor bank were not met. Lastly, the new circuitry was installed onto the system architecture and automation testing of the SS-CAES was carried out throughout the day.

1. Benchtop Testing of New Power Supply Circuitry

Figure 27 shows the setup of the power supply module circuitry for benchtop testing. A total of two power supply modules were set up. On the PLC signal circuit, one power supply module was set up to send a 24 VDC signal to the PLC to simulate that the conditions of the voltages of the capacitor bank were not met and the SSR would need to be activated. On the capacitor charging circuit, a second power supply module was set up to charge the supercapacitor.
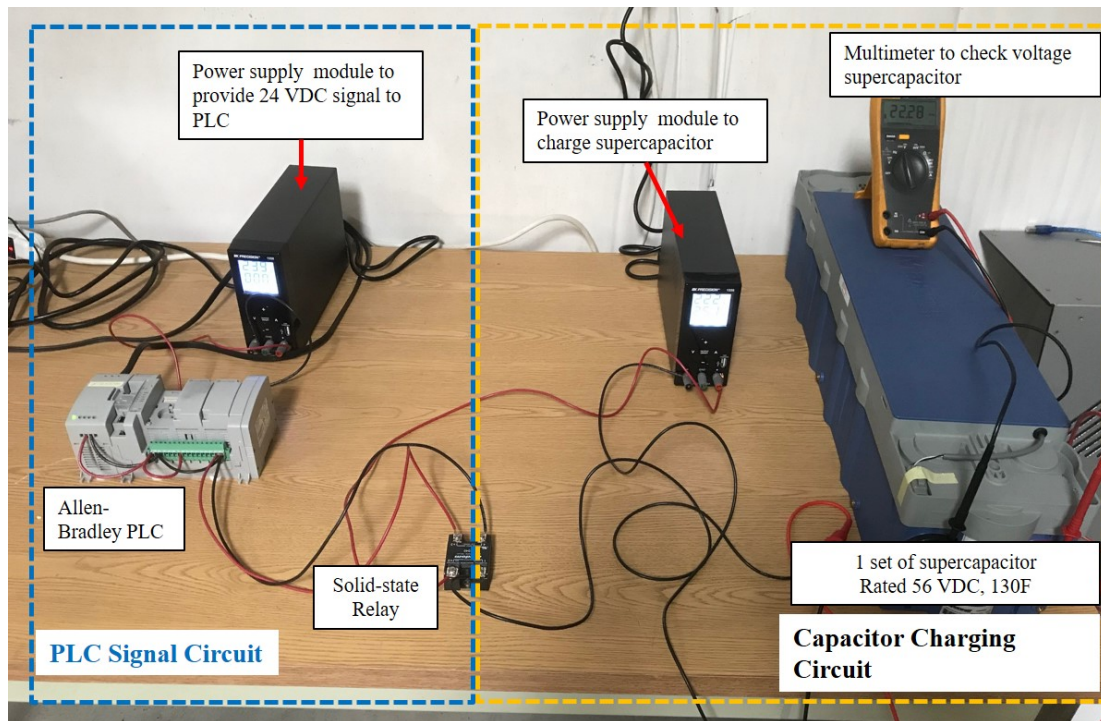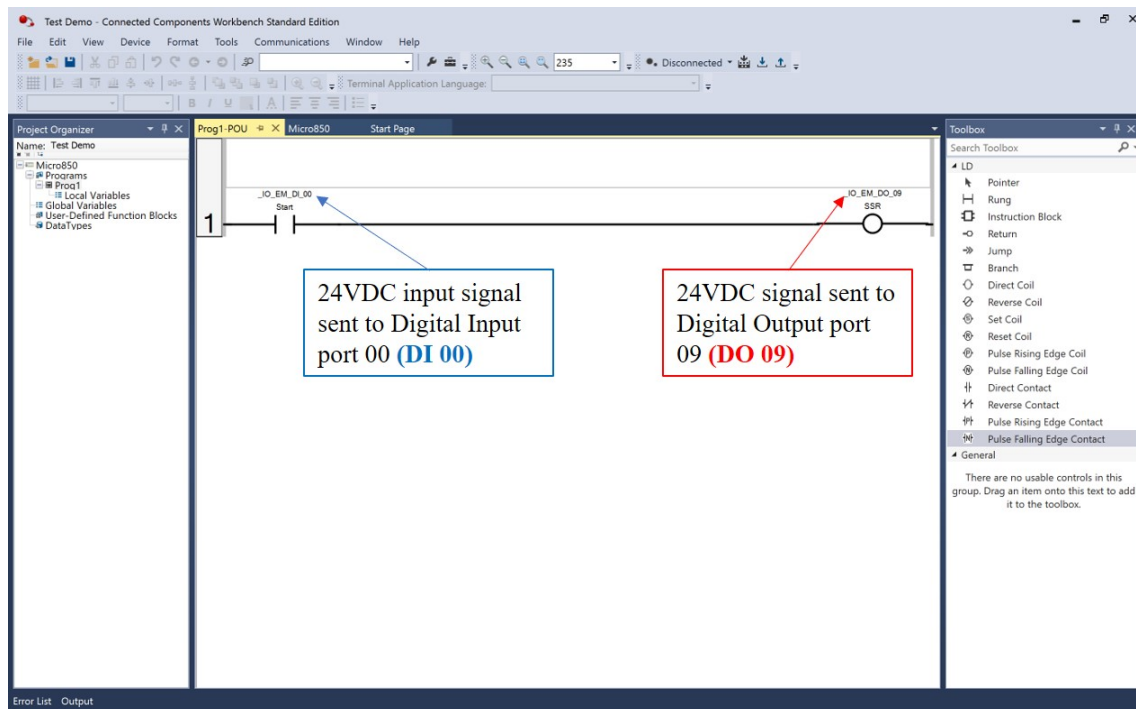
Figure 27.　Setup for Benchtop Testing

Figure 28.　Ladder Diagram Program for Benchtop Testing

A ladder diagram (LD) program was written to automate the supercapacitor charging process by the PLC, SSR and power supply module. Figure 28 shows the LD program written for this benchtop testing. The benchtop testing provided a few key observations. Firstly, the automated control of the power supply by the module to the common bus via the SSR, was confirmed to be feasible. Secondly, the power supply module was able to provide a maximum output voltage of 36.8 VDC and a maximum current output of 3.38A when connected to the capacitor charging circuit.

Thirdly, the time recorded to charge a 130F capacitor bank was approximately 3 minutes. Based on extrapolation, this would mean that the time needed to charge the six sets of capacitor bank with a total capacitance of 780F, would be approximately 18 mins. In the program written by Williams, he had allocated a delay time of 10 mins for the compressor to be started after sunset. The delay time was enforced to ensure that the capacitor bank have enough power for the simultaneous operation of the inverter and compressor. Therefore, there would be a need to increase the delay time for the restart of the compressor after sunset from 10 to 20 minutes.

Lastly, rapid cycling test was also conducted on the active PLC charging circuit to determine the response of the power supply module. The capacitor bank was discharged with a resistor from 36 VDC to 33 VDC, for five runs. For all the runs, the power supply module was able to cut in immediately and recharge the capacitor bank to 36 VDC.

2.   **Programming the Sub-routine to Integrate the Activation of Power Supply Module**

Figure 29 shows the program written in the Connected Components Workbench software, to activate the power supplied to the common bus by the power supply module when the capacitor voltage falls below 33VDC. The description of various segments of the code could be found in the appendix.

The codes were made up of two key segments. The first segment consisted of a comparator function block that would determine if the raw capacitor voltage retrieved from the MPPT charge controller via the Modbus was less than 33VDC. If the capacitor voltage was determined to be less than 33VDC, the PLC would energize the output signal port

DO_09 that is connected to the SSR. Subsequently, the capacitor charging circuit would be activated.

The second segment consisted of a comparator function block that would determine if the voltage across the capacitor had reached at least 36VDC so that the power supply from the module could be deactivated by de-energizing the digital output port DO_09. This second comparator was incorporated to protect and prevent the power supply module from operating beyond its safe working range.
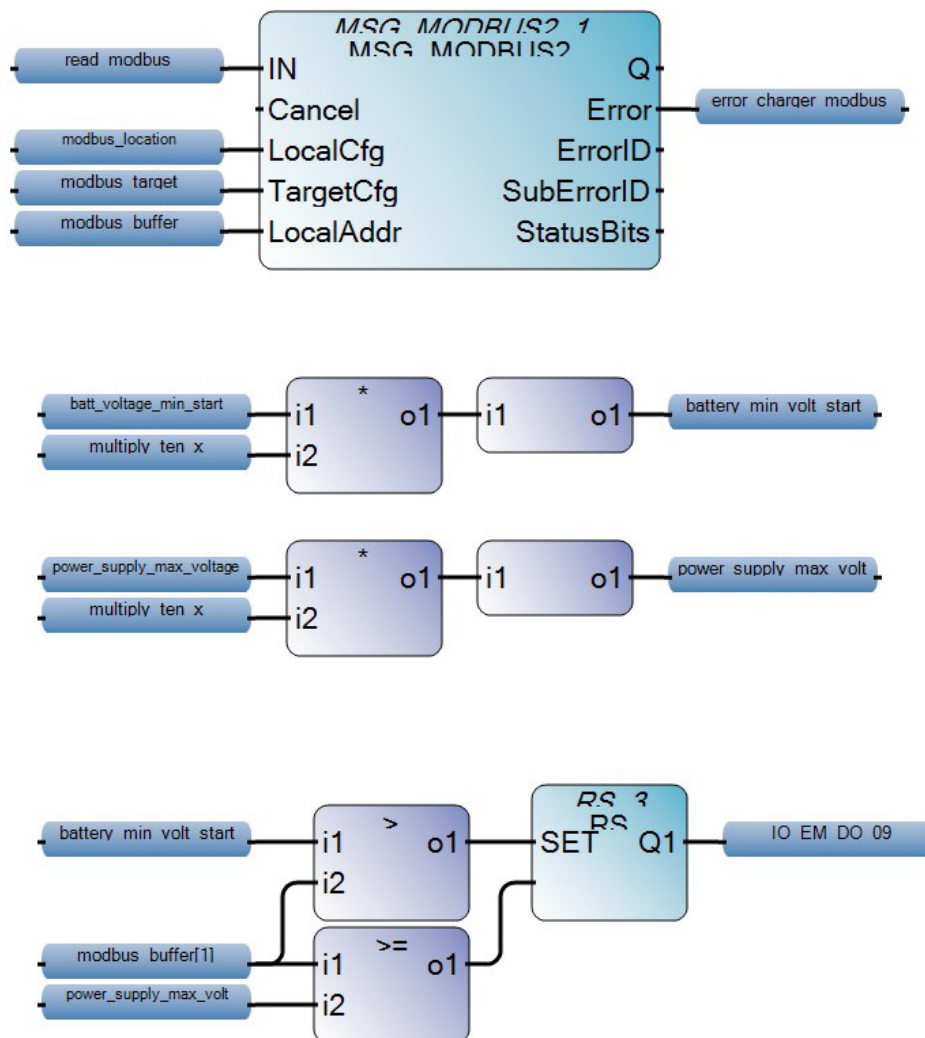

Figure 29.   Program to Activate Power Supply Module

3. Actual Setup

This section shows the actual setup of the SS-CAES (electrical components side) with the newly integrated power supply module circuitry.
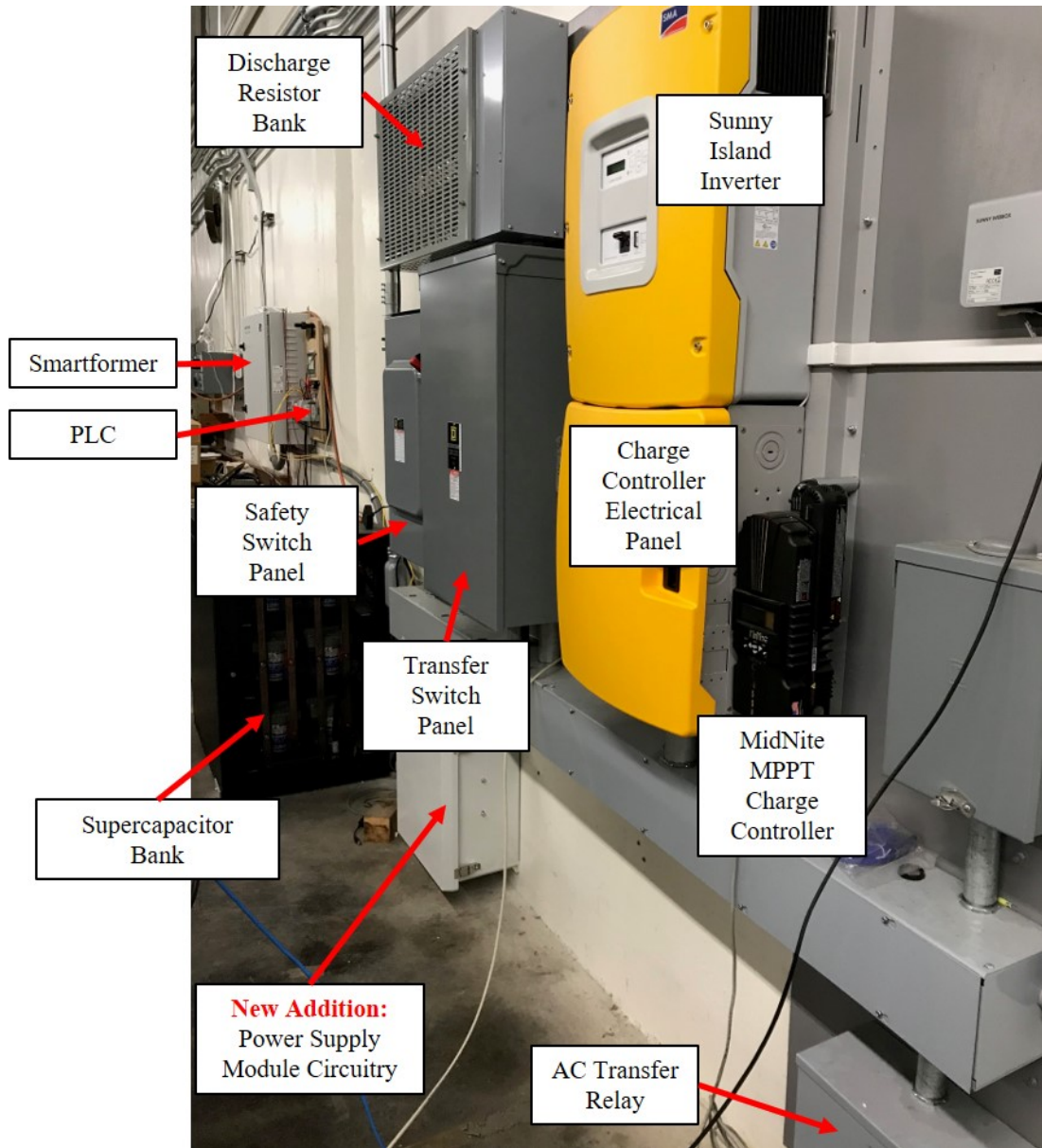

Figure 30. SS-CAES Electrical System Architecture with Integrated
Power Supply Module

Figure 31 shows the setup and wiring inside the power supply circuitry box. A hole was drilled near the exhaust end of the power supply module to provide ventilation and allow access for the electrical cable.
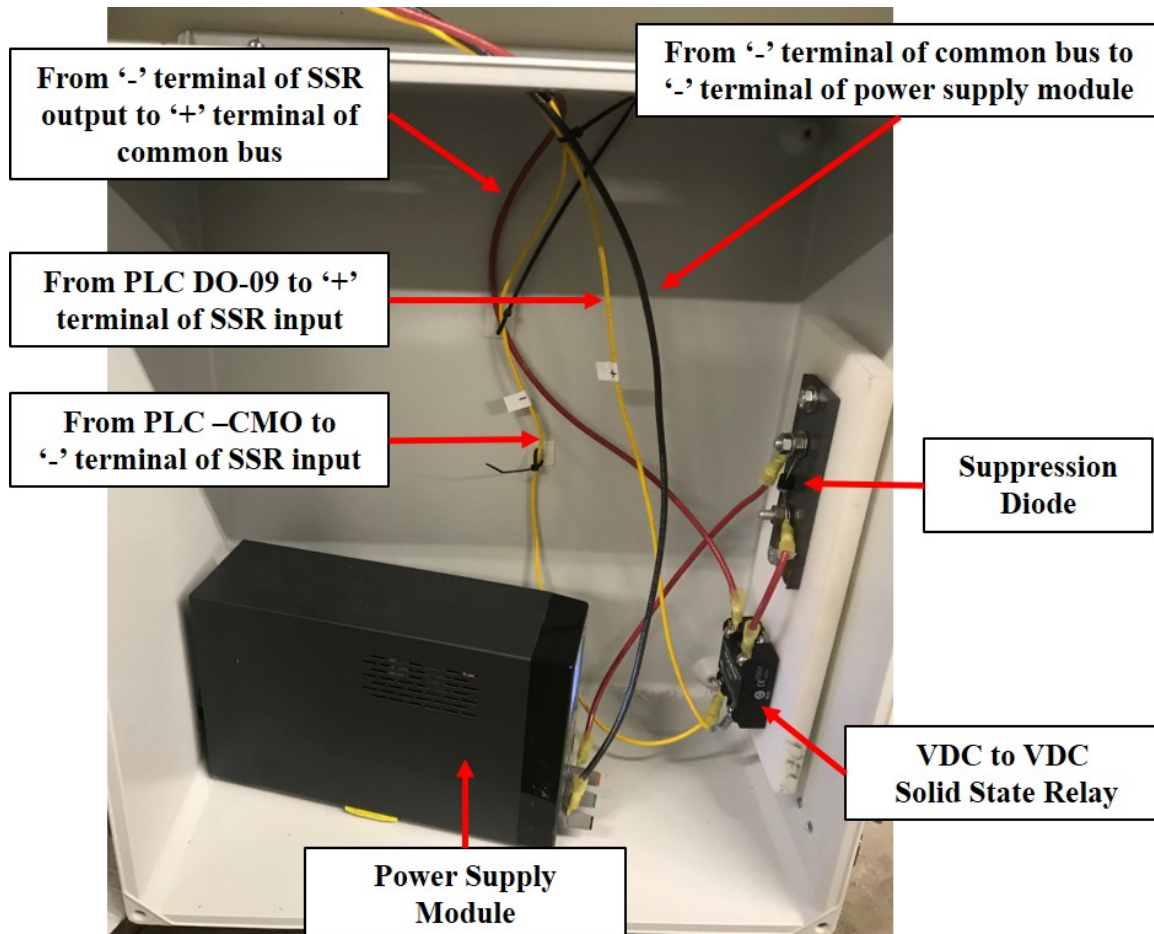

Figure 31. Power Supply Module Circuitry

Figure 32 shows the connection of the wirings from the power supply module to the common bus in the charge controller electrical panel.
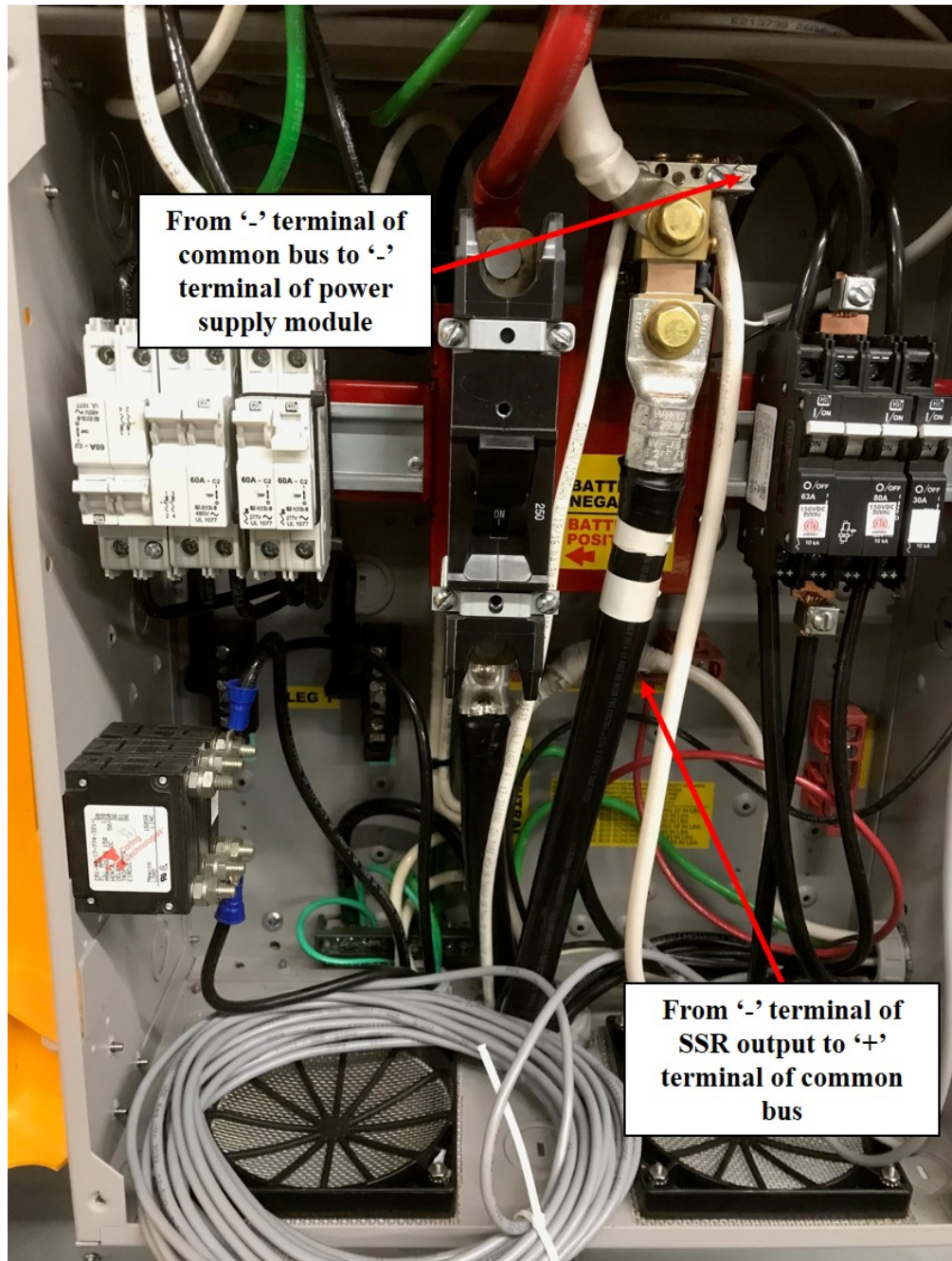

Figure 32.   Charge Controller Electrical Panel Wiring

Figure 33 shows the wiring of the PLC to integrate the power supply module circuitry. The new wiring plan would have three embedded digital output ports being utilised. DO-00, DO-01 and DO-09 were allocated for the activation of the air compressor, air dryer and SSR, respectively.
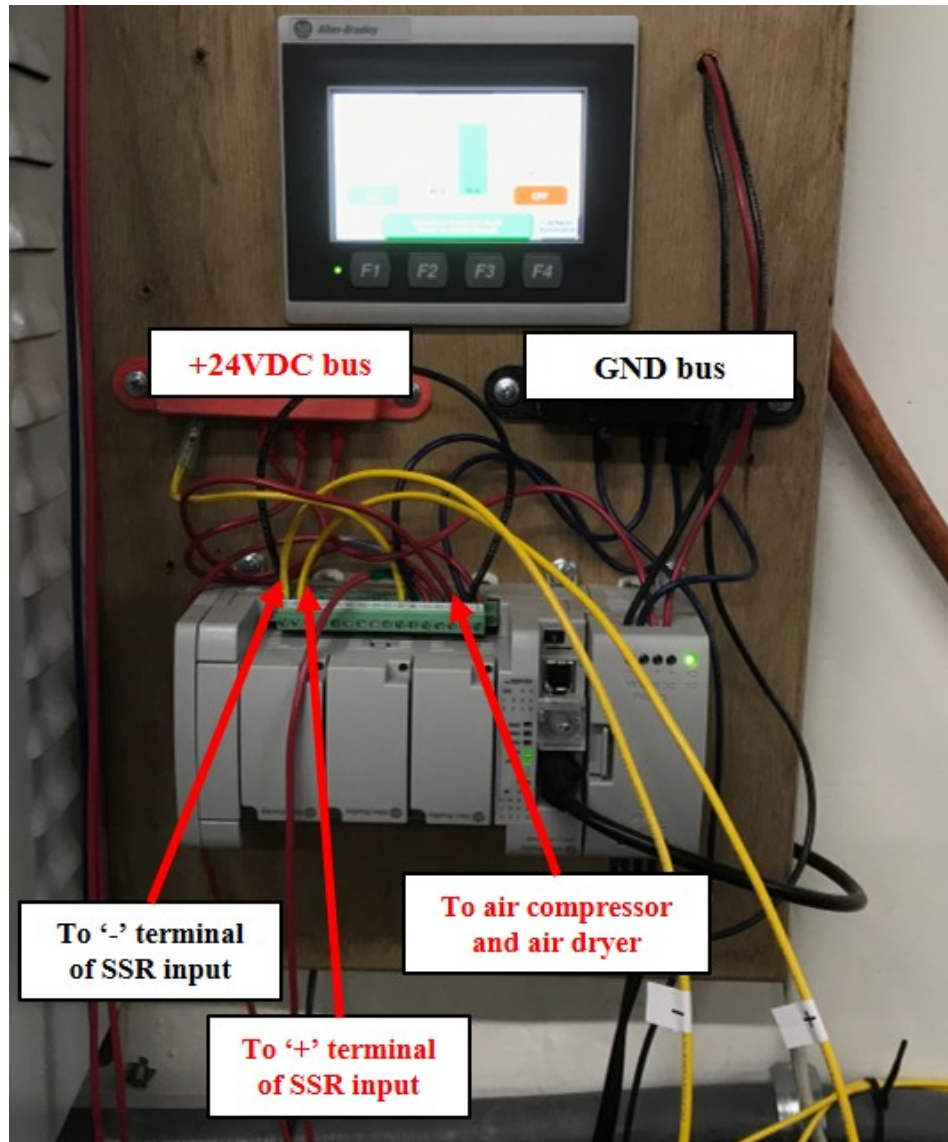

Figure 33.   PLC Wiring to Integrate Power Supply Module Circuitry

D.   RESULTS

A full-scale testing of the SS-CAES integrated with the power supply module was conducted and the system parameters were recorded by the Modbus. Figure 34, 35 and 36 would present data to show that the automated SS-CAES was in active operation throughout the period of full-scale testing.

Figure 34 shows the capacitor bank voltage data recorded during the active operation of the automated SS-CAES for a period of four days. The cycling of the capacitor voltages would refer to the periods when the PV array was generating electricity and the air compressor was in active operation. The PV array would generate electricity to charge the capacitor bank while the operation of the air compressor would reduce the capacitor bank voltage. The steady capacitor bank voltages would refer to the periods when the power supply module maintained the capacitor bank voltage at 36VDC after sunset.
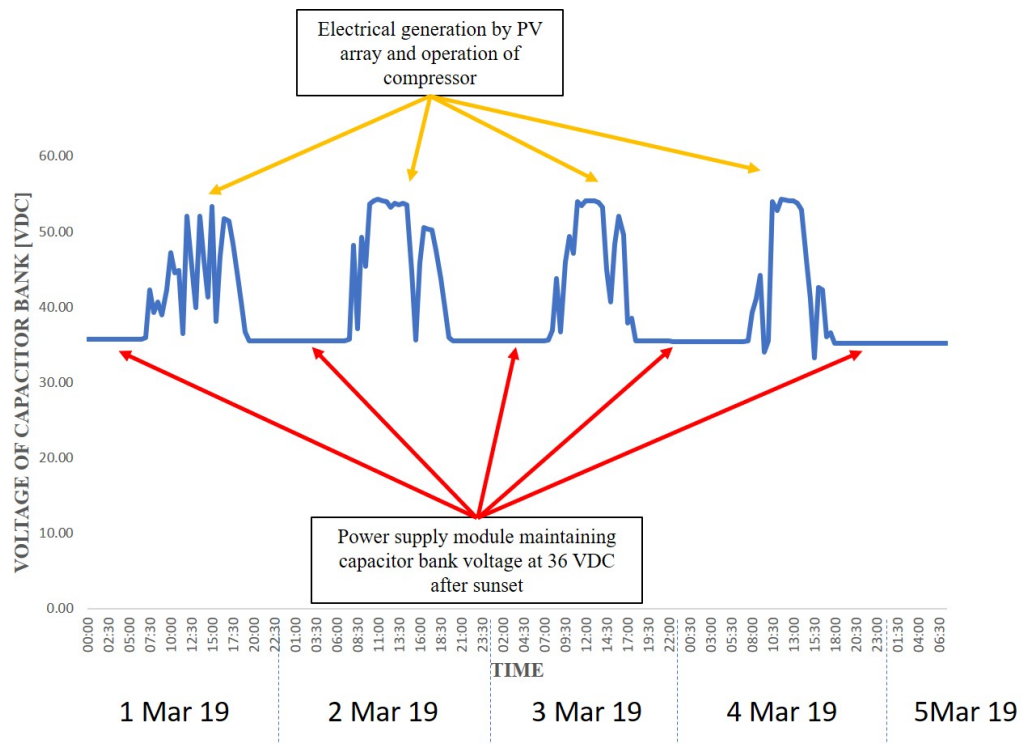

Figure 34.   Capacitor Bank Voltage Data from 1–5 March 2019

Figure 35 shows the inverter current data recorded during the full-scale testing. The spikes in the inverter current data would refer to the periods when the inverter had to supply current for the operation of the air compressor. The highest inverter current data recorded occurred when the air compressor was first started to charge an empty air storage bottle. The steady inverter current data recorded would refer to the active operation of the inverter after sunset.
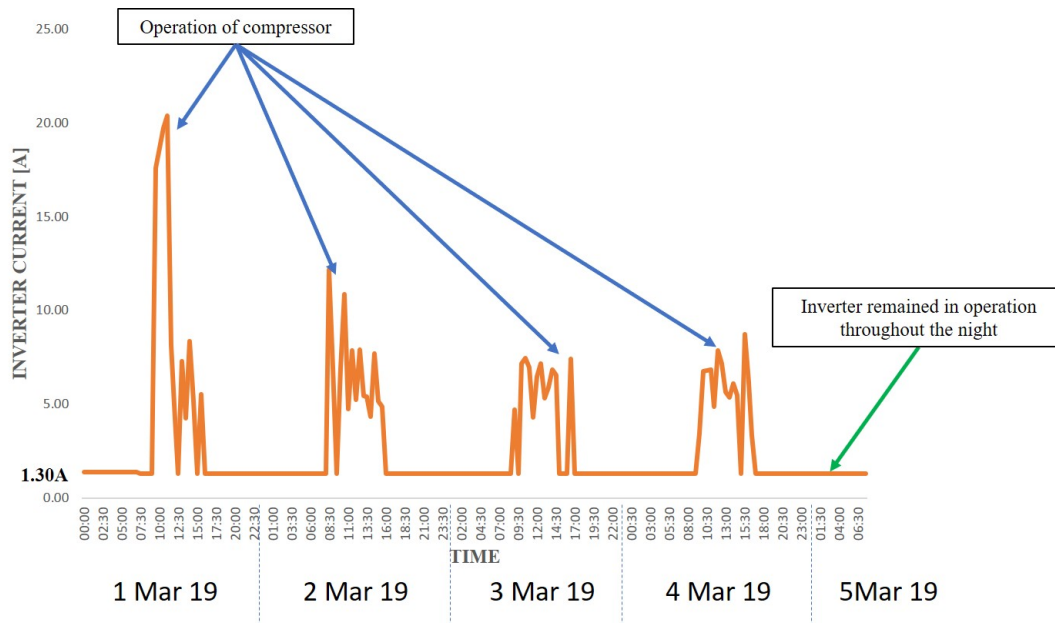

Figure 35.   Inverter Current Data from 1–5 March 2019

Figure 36 shows a magnified view of the capacitor voltage data recorded throughout the night on 5 March 19. From the data, the power supply module was observed to charge the capacitor bank when the voltage drops to 33 VDC and was deactivated when the voltage exceeded 36 VDC. From the data, it was also observed that there was an approximate drop of 1 V between the power supply module and the capacitor bank. The difference in the voltage supplied by the power supply module and the capacitor bank voltage could be due to resistance losses in the wiring and voltage drop across the diode.
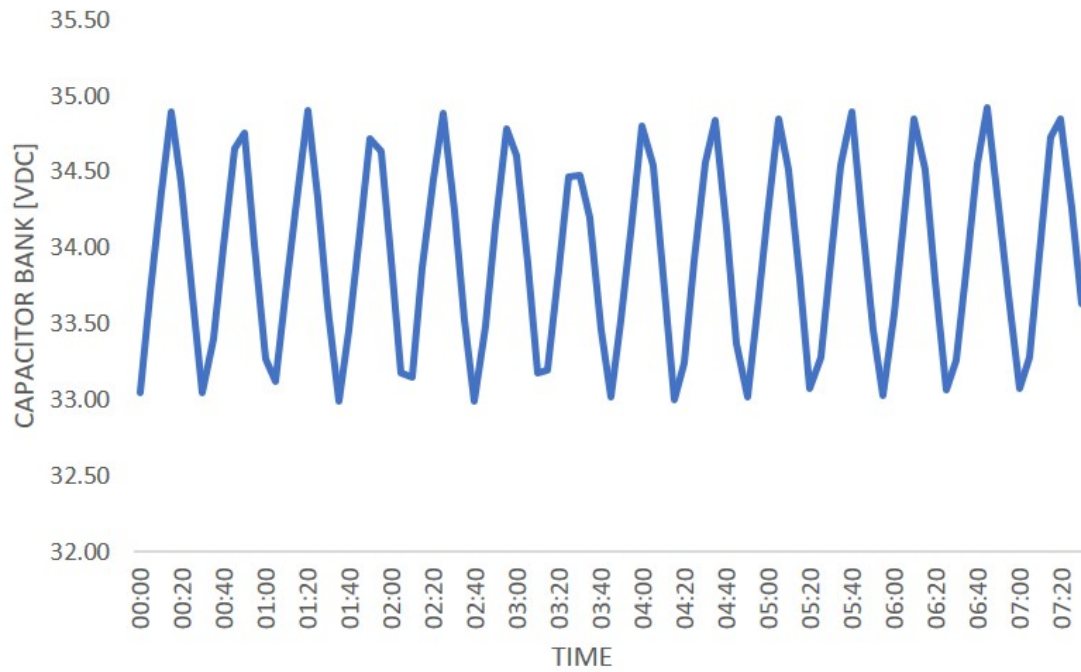
Figure 36. Cycling Capacitor Bank Voltage Data on 5 March 2019

THIS PAGE INTENTIONALLY LEFT BLANK

V.   CONCLUSION AND RECOMMENDATIONS

The aim of the thesis to provide a proof-of-concept for an automated industrial control of SS-CAES had been achieved. With the integration of the power supply module circuitry, the automated SS-CAES maintained active operation, even when the PV array stopped electrical generation. The automated SS-CAES was also able to charge and maintained the pressure of the compressed air tank at 793 kPa (115 PSI).

The demonstration of the automated SS-CAES would mean that the system was ready for trial and implementation across identified military installations. The automated SS-CAES would greatly aid the Navy's transition to renewable energy sources for military installations.

There are several recommendations to further enhance the NPS-IMPEL SS-CAES:

- When the expansion and compression systems of the SS-CAES are fully integrated, the power supply module can still be utilised as a form of backup power to the solar microgrid.

- The setup of PLC signal circuit and capacitor charging circuit can be utilised to facilitate the benchtop testing of the compressed air generator before the actual installation and integration to the microgrid. The VDC output end of the air-driven generator can be easily connected to the capacitor charging circuit to conduct benchtop testing to determine if the air-driven generator is able to charge the capacitor.

- The current SS-CAES system architecture does not have any capability to remotely monitor the pressure levels of the compressed air tanks as there are no pressure sensors installed. The ability to remotely monitor the tank pressure will allow the SS-CAES to control the activation of the air compressor based on pressure inputs. However, this will require substantial work in terms of installing and wiring pressure sensors on the input and output piping of the tanks to the PLC.

THIS PAGE INTENTIONALLY LEFT BLANK

APPENDIX. DETAILS OF PROGRAM AND INSTALLATION

For the purpose of knowledge retention, this appendix will contain details on setting up the controller for the first time, programming of the controller, description of the program written to integrate the activation of the power supply module and details of wiring to integrate the power supply module circuitry to the overall system architecture.

A.   SETTING UP THE CONTROLLER FOR THE FIRST TIME

1.   Overview of the Connected Component Workbench Software

The Connected Component Workbench software can be downloaded from the Rockwell Automation website. Figure 37 and 38 provide an overview of the key features and functions of the Connected Component Workbench software.
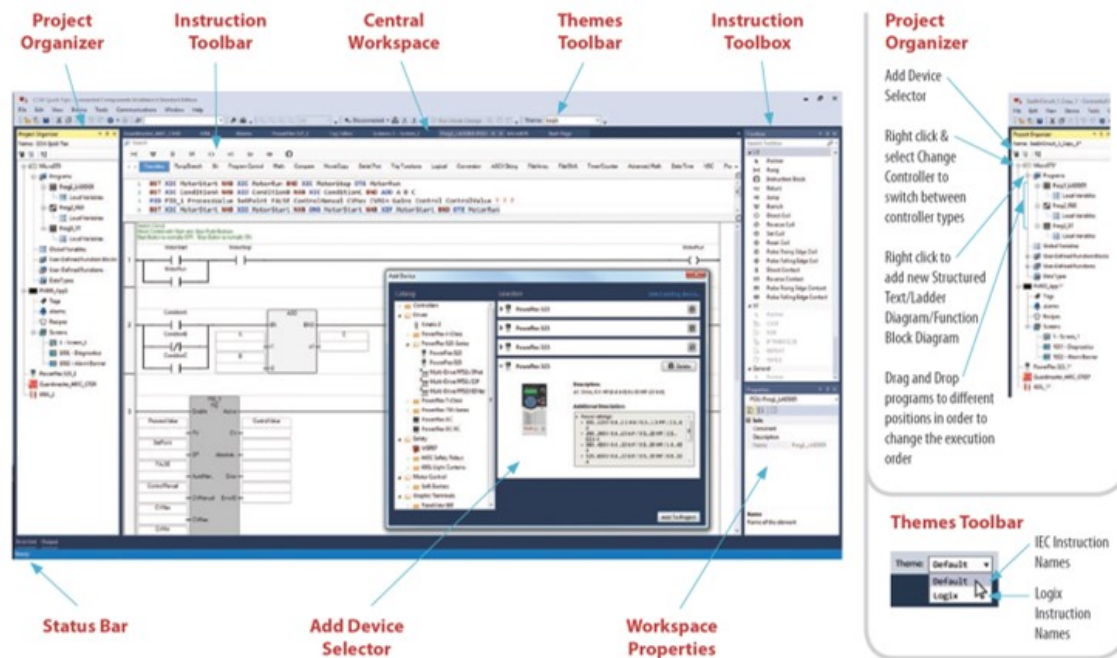

Figure 37.   Key Features of the Connected Components Workbench
Project Space. Source: [38].

Figure 38.   Key Functions of Connected Components Workbench
Software. Source: [38].

2.   Uploading the Existing Program from the PLC for the First Time

In the PLC programming terms, to upload will refer to uploading the program from the controller to your computer and to download will refer to downloading the program in your laptop to the controller. The most convenient method to perform the uploading will be to connect the computer to the PLC with the USB Type B cable:

- Launch the Connected Component Workbench software.

- Click on 'Discover' and choose the Micro850 Automated CAES as shown in Figure 39.

- Click on the upload button at the toolbar and the program in the PLC will be downloaded into your computer. You can then save the file into any designated folder.
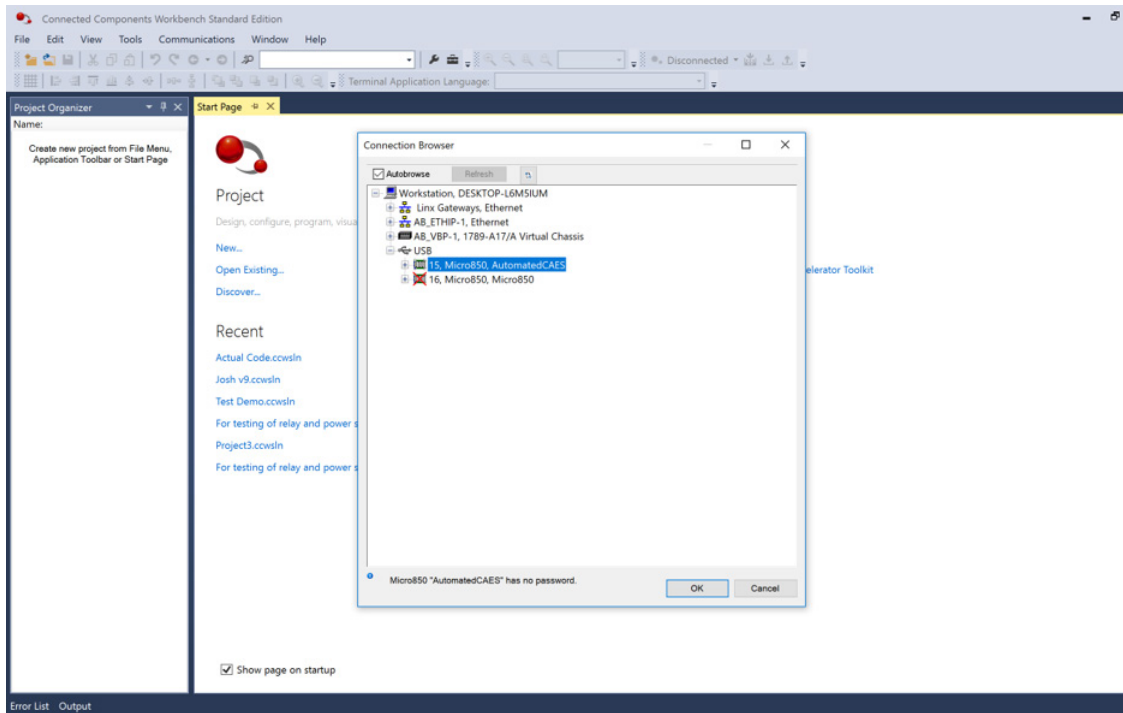
Figure 39.   Connection Browser

3.   Creating a New PLC Project

- Click on 'New' on the start page and name the new project as shown in Figure 40.

- Choose the Micro850-LC50-24QBB on the 'Controller' tab and select 'Version 9' for its firmware as shown in Figure 41.

- Once the controller is selected and added to the project, the Micro850 home page would be launched. Set up the internet protocol (IP) address as shown in Figure 42.
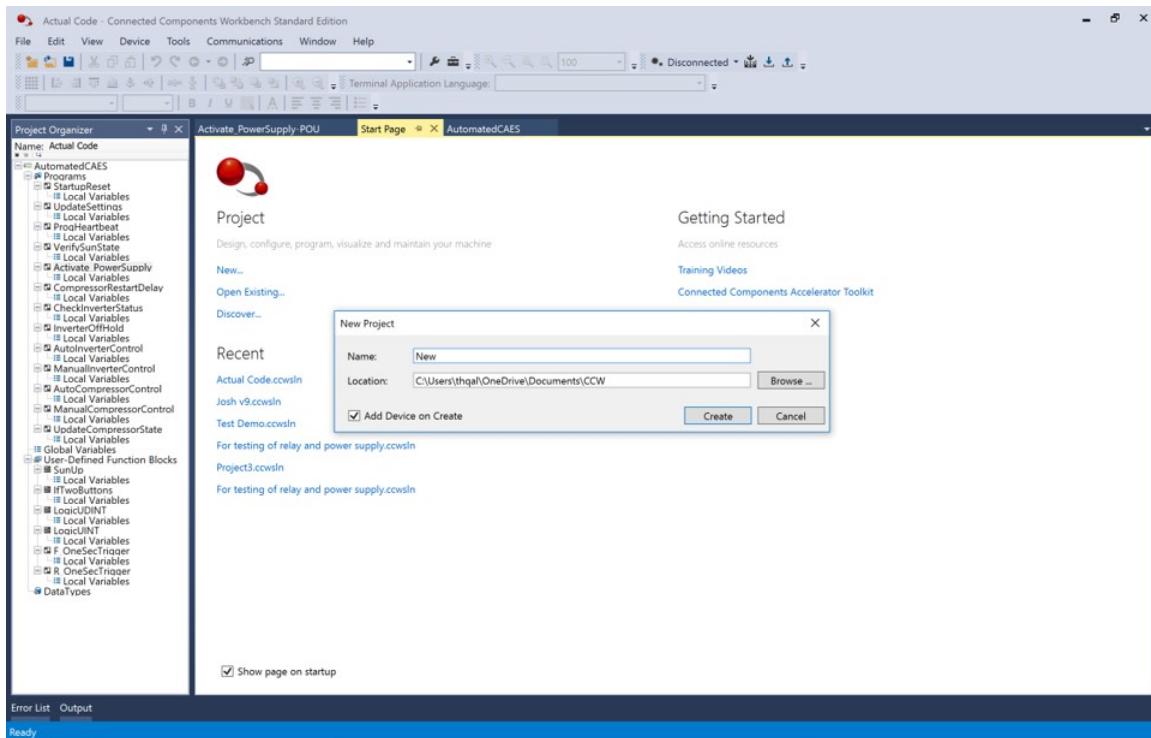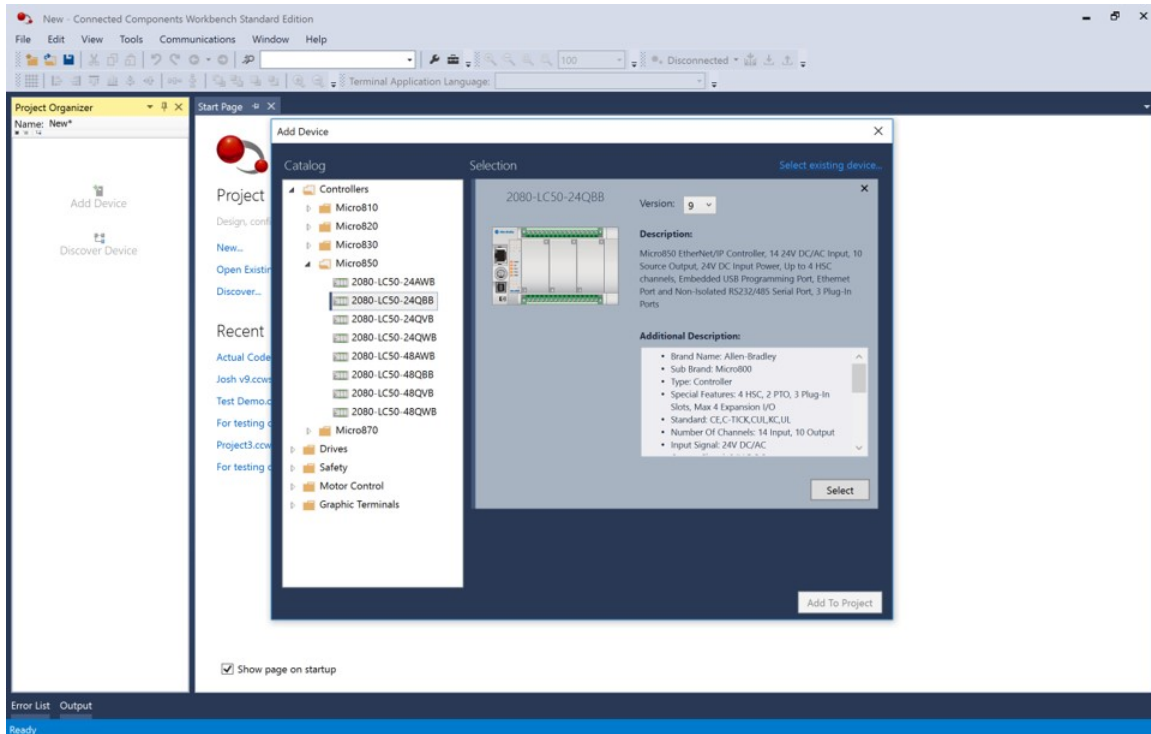
Figure 40.   Creating New Project

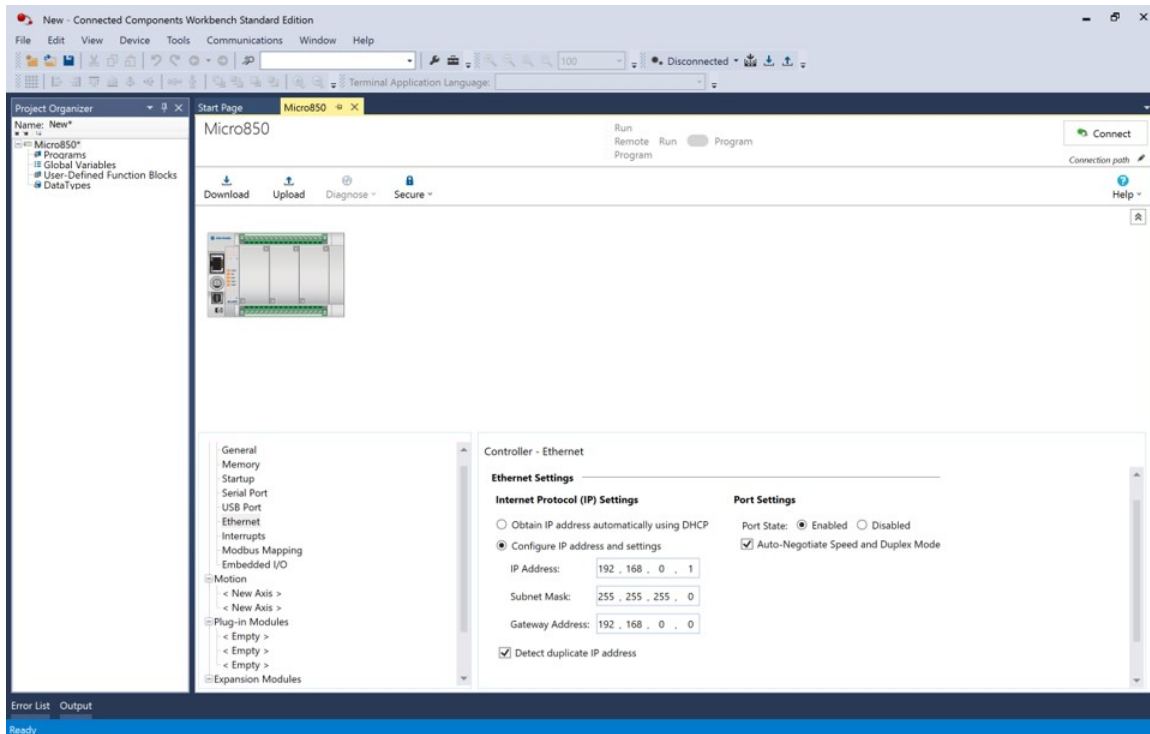Figure 41.   Selection of Micro850 on the Add Device Page

Figure 42.   Setting up the IP settings for the SS-CAES Micro850 PLC

B.   BASIC PROGRAMMING OF THE PLC

Figure 43 shows the online courses on the Udemy website, that I had taken, to learn the fundamentals of industrial automation and generic PLC programming. The various courses introduced basics such as programming logics and hardware wiring of the PLC to sensors and motors. References [39], [40], and [41] are online user manuals that were sourced online that could provide some free and basic guides to programming the Micro850 PLC.

Ladder Diagram, Function Block Diagram and Structured Text are the three common methods to program the PLC. Ladder Diagrams are ideal for programs with sequential processes and require minimal Boolean operations. Function Block Diagrams are more ideal for programs which require concurrent and complex Boolean operations. Structured Text are ideal for programs that require very complex Boolean operations. Figure 44 provides an example of a Ladder Diagram method. Figure 45 shows an example of a Function Block Diagram method. Figure 46 shows an example of the Structured Text

method. The instructors of the online courses on Udemy would offer projects and guides to aid students in programming the PLC using the 3 different methods.
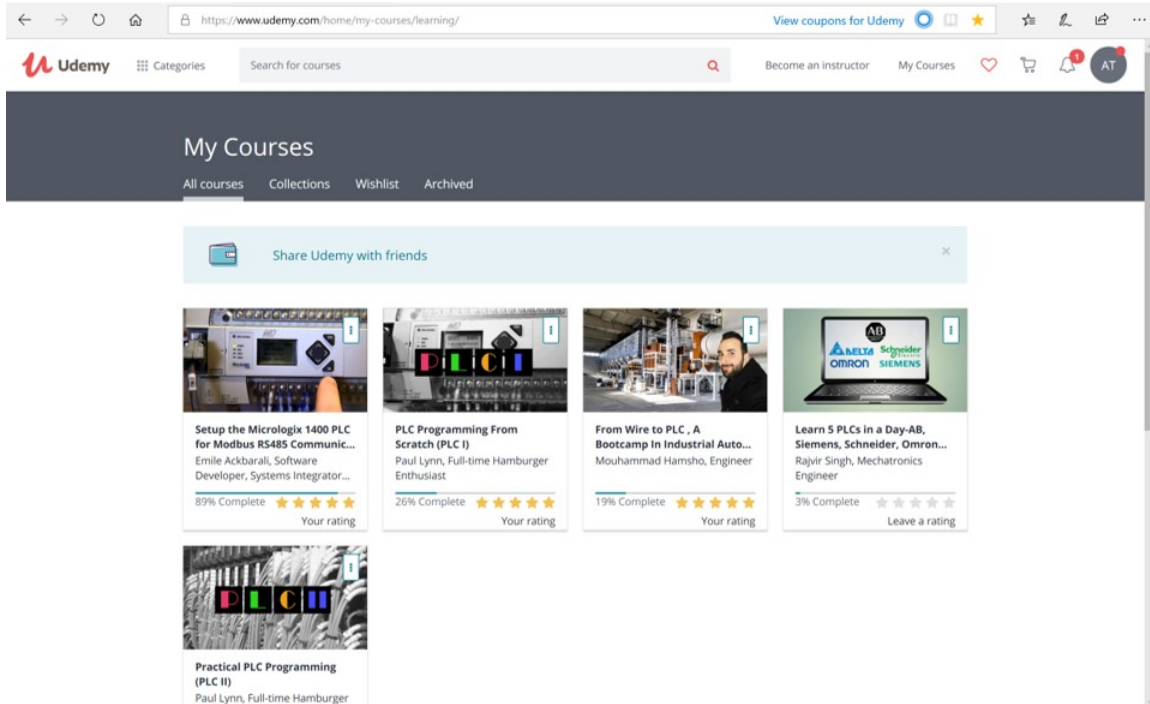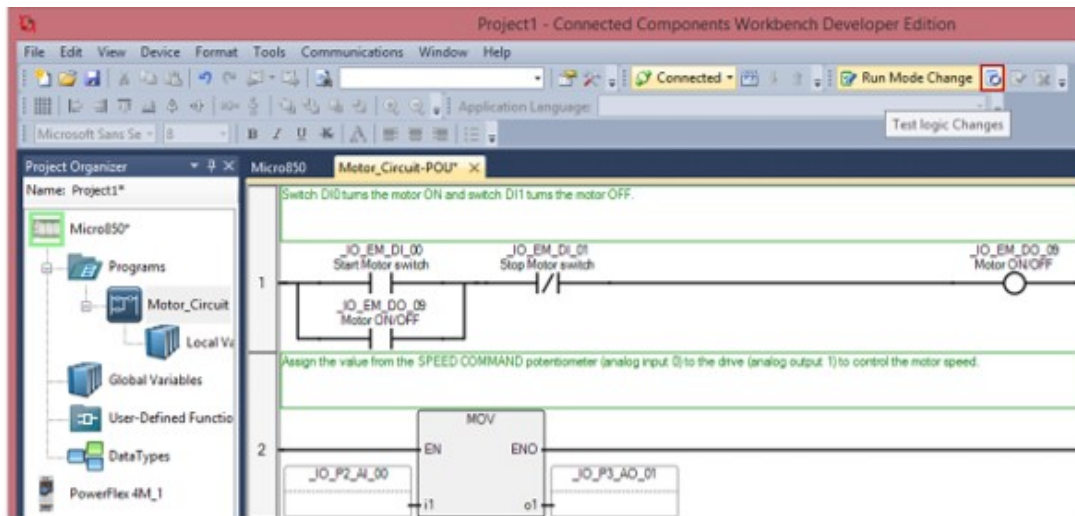

Figure 43.   Online Courses on Udemy

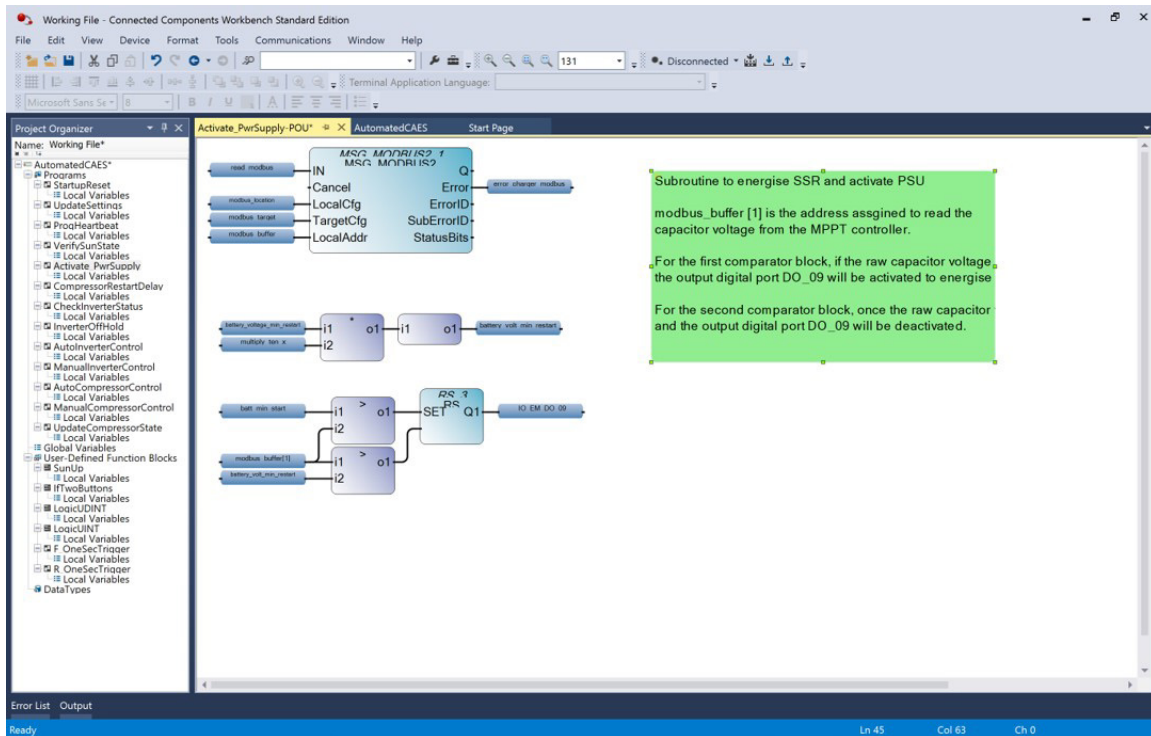Figure 44.   Example of Ladder Diagram. Source: [39].

Figure 45.   Example of Function Block Diagram

Figure 46.   Example of Structured Text. Source: [8].

C.   DESCRIPTION OF THE ACTIVATE POWER SUPPLY PROGRAM

Figure 47 shows the breakdown and description of the three main segments of the program to activate the power supply module.
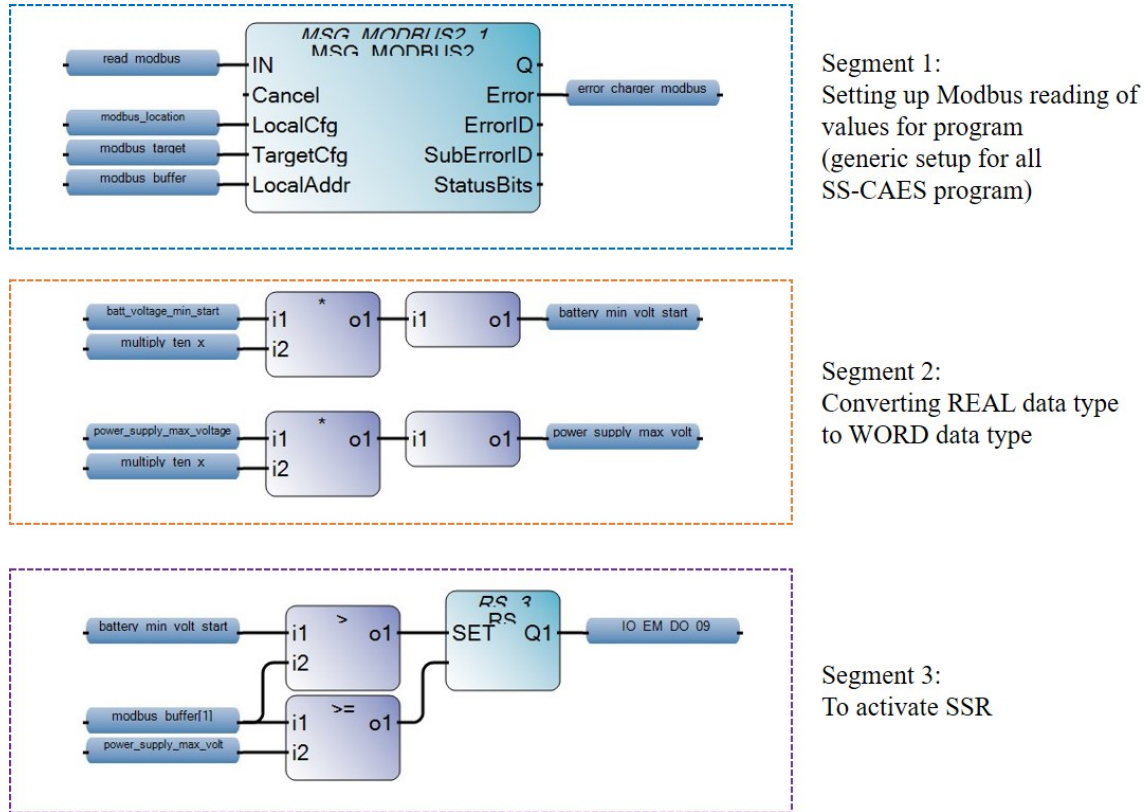
Figure 47.   Description of Program to Activate Power Supply Module

The first segment was a generic setup for the program to read values from the Modbus gateway. For new programs that would require reading data from the Modbus, this segment would need to be set up.

The second segment was to convert the global variables '*batt_voltage_min_start*' and '*power_supply_max_voltage*' from REAL data type to WORD data type. The comparator blocks in segment 3 would only be able to compare data of the same data types. As data from the Modbus would be in WORD data type, the conversion was required to convert the REAL values set in the global variables to WORD data types.

The third segment would be the actual setup to energize or de-energize the digital output IO_EM_DO_09 so that the connected SSR could be activated or deactivated, respectively.

The first comparator block at the top would compare the preset capacitor bank voltage (battery_min_volt_start set at 33.0 VDC) against the actual capacitor bank voltage pulled from the Modbus (modbus_buffer[1]). If the preset voltage of 33.0 VDC was more than the actual voltage, the condition would be met and the digital output 09 would be 'SET' and energised.

The second comparator block was set up to de-energize the digital output. It would compare the actual capacitor bank voltage pulled from the Modbus (modbus_buffer[1]) against the preset capacitor bank voltage (power_supply_max_voltage set at 36.0 VDC). If the actual voltage was more than or equal to the preset voltage of 36.0 VDC, the condition would be met and the digital output 09 would be 'RESET' and de-energised.

D.   GLOBAL VARIABLES

Table 4.   Global Variables

Variable Name	Data Type	Initial Value
power_supply_max_voltage	REAL	36.0
battery_voltage_min_start	REAL	33.0
min_restart_time	REAL	20.0
battery_volt_min_restart	WORD	400
power_supply_max_volt	WORD	360
IO_EM_DO_09	BOOL	FALSE

E. LOCAL VARIABLES

Table 5.   Local Variables

Variable Name	Data Type	Initial Value
MSG_MODBUS2_1	MSG_MODBUS2	
modbus_buffer	MODBUSLOCADDR	
modbus_location	MODBUS2LOCPARA	
- Channel	UINT	4
- TriggerType	UDINT	10000
- Cmd	USINT	3
- ElementCnt	UINT	2
modbus_target	MODBUS2TARPARA	
- Addr	UDINT	4115
- NodeAddress	MODBUS2NODEADDR	
- NodeAddress[0]	USINT	192
- NodeAddress[1]	USINT	168
- NodeAddress[2]	USINT	0
- NodeAddress[3]	USINT	50
Port	UINT	0
UnitID	USINT	1
MsgTimeout	UDINT	0
ConnTimeout	UDINT	0
CommClose	BOOL	TRUE
read_modbus	BOOL	TRUE
multiply_ten_x	REAL	10

F. WIRING DEVICES TO THE EMBEDDED DIGITAL INPUT AND OUTPUT PORTS

For digital inputs,
- 24VDC connected to CMO port
- 0VDC connected to the tagged input port I-xx

For digital outputs,
- 24VDC connected to CMO port
- CMO port to positive terminal of output device
- Tagged output port O-xx to negative terminal of output device

To + terminal of output device

To - terminal of output device
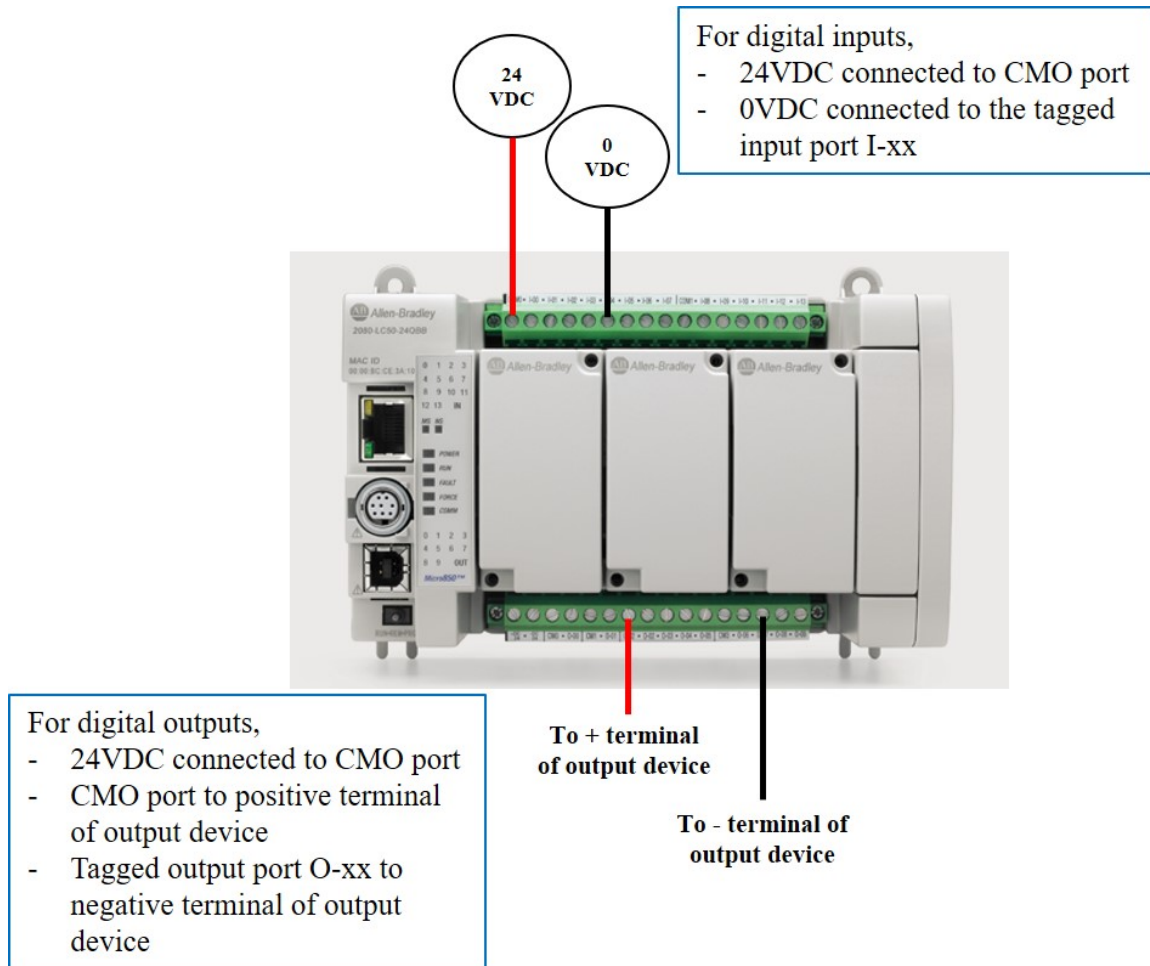
Figure 48.   Wiring of PLC to Digital I/O Devices

G. WIRING THE PLC SIGNAL CIRCUIT AND THE CAPACITOR CHARGING CIRCUIT

Figure 49. Overview of Wiring of PLC Signal Circuit and Capacitor Charging Circuit

H. WIRING OF CHARGE CONTROLLER ELECTRICAL PANEL

From '-' terminal of common bus to '-' terminal of power supply module

From '-' terminal of SSR output to '+' terminal of common bus

Figure 50.   Wiring in the Charge Controller Electrical Panel

Figure 51.   Wiring Schematics of Charge Controller Electrical Panel

LIST OF REFERENCES

[1]   U.S. Department of Energy, n.d., "Comprehensive Annual Energy Data and Sustainability Performance." [Online]. Available: http://ctsedwweb.ee.doe.gov/ Annual/Report/Report.aspx

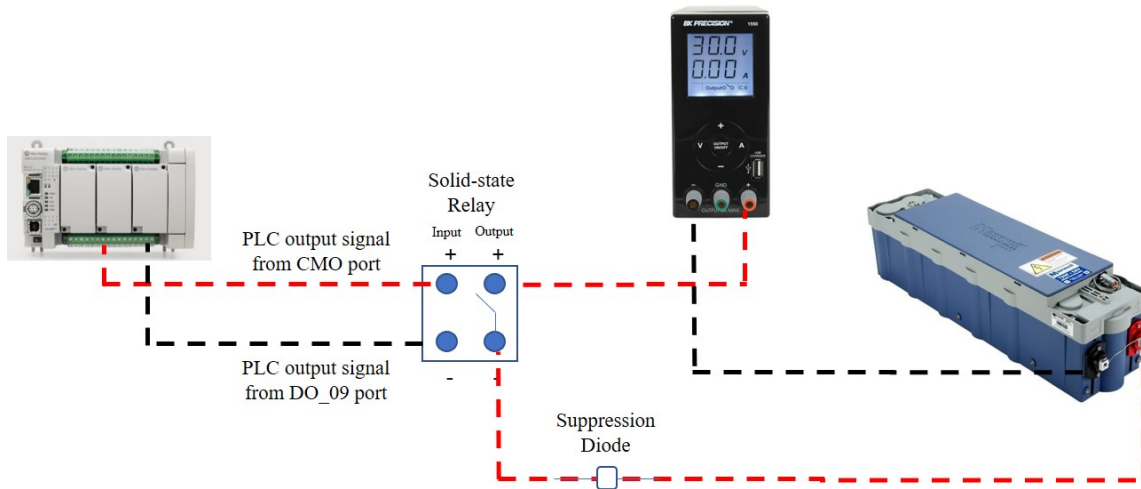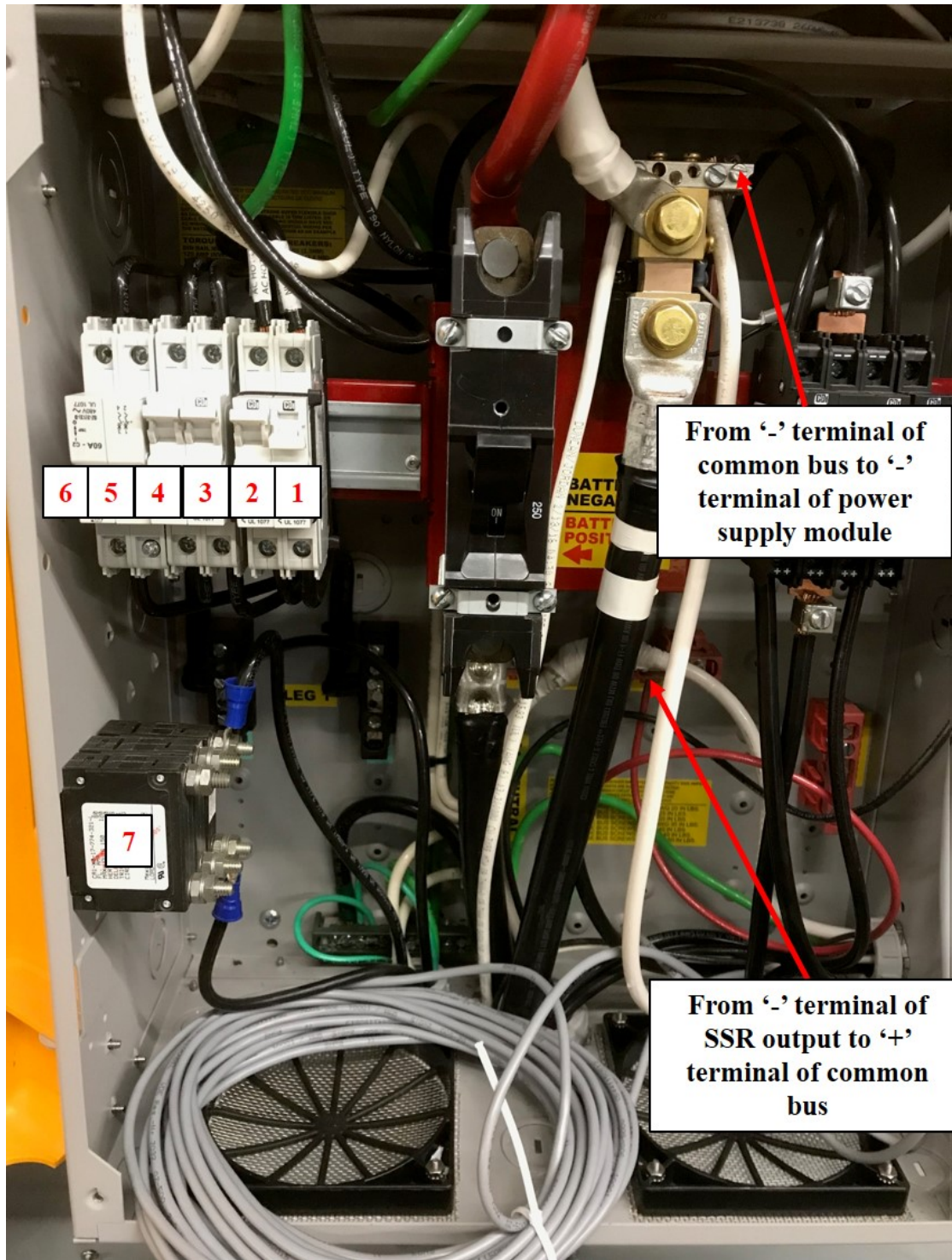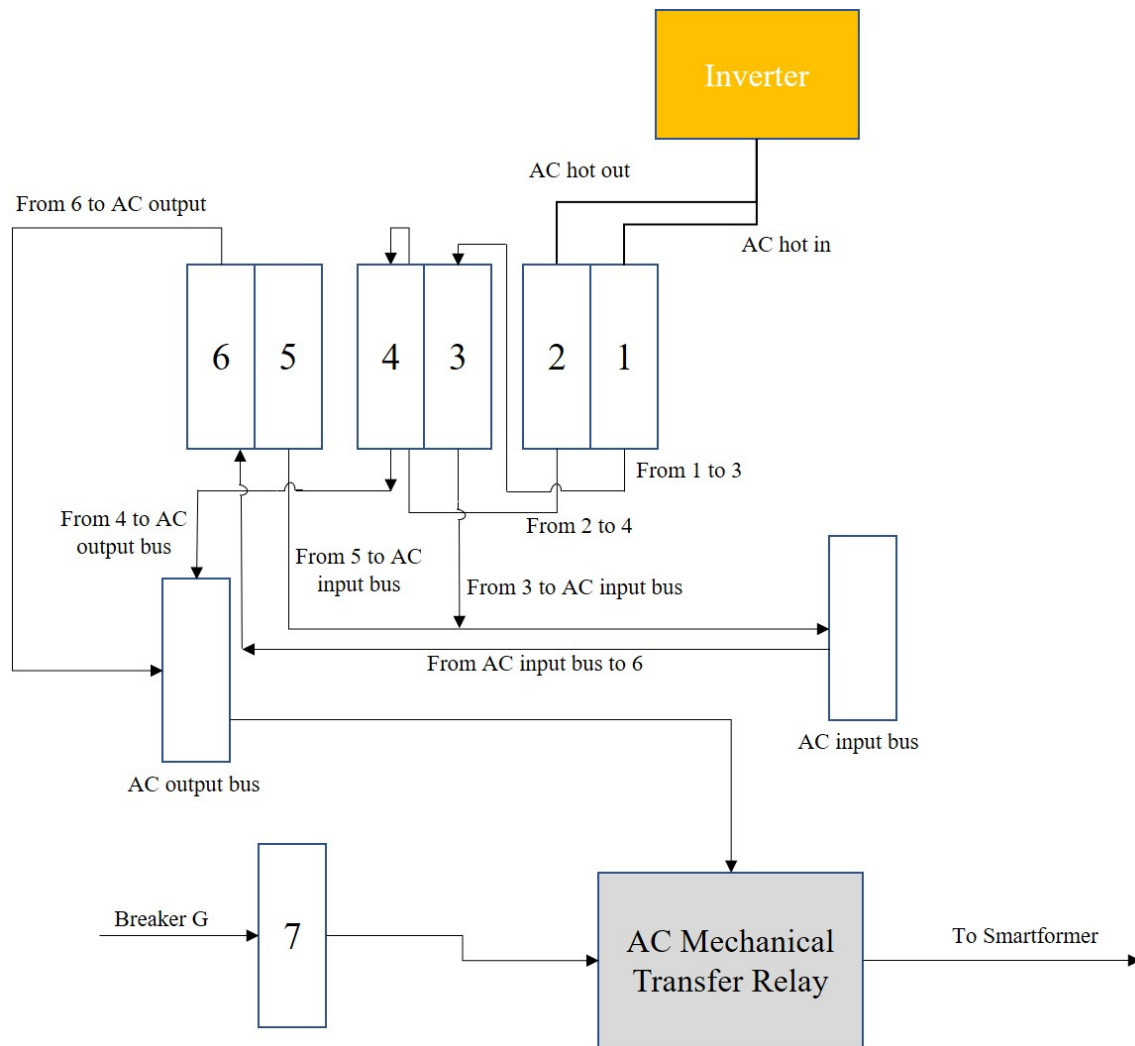[2]   Department of the Navy, n.d., "Energy Program for Security and Independence." [Online]. Available: https://www.secnav.navy.mil/eie/ASN%20EIE%20Policy/ Naval_Energy_Strategic_Roadmap.pdf

[3]   Petrov, P. P., Arghandeh, R., and Broadwater, R., 2013, "Concept and Application of Distributed Compressed Air Energy Storage Systems Integrated in Utility Networks," ASME 2013 Power Conference, Boston, pp. 1-4.

[4]   Center for Sustainable Systems, University of Michigan, n.d., "U.S. Grid Energy Storage Factsheet." [Online]. Available: http://css.umich.edu/factsheets/us-grid-energy-storage-factsheet

[5]   Mclaughlin, C. S., 2016, "Small-scale Air-driven Generator," M.S. thesis, Dept. of Mech. and Aero. Eng., Naval Postgraduate School.

[6]   Prinsen, T. H., 2016, "Design and Analysis of a Solar-powered Compressed Air Energy Storage System," M.S. thesis, Dept. of Mech. and Aero. Eng., Naval Postgraduate School.

[7]   Vranas, T. M., 2017, "Control System Development for Power Generation from Small-Scale Compressed Air Energy Storage," M.S. thesis, Dept. of Mech. and Aero. Eng., Naval Postgraduate School.

[8]   Williams, Joshua N. 2017, "Automated Control of a Solar Microgrid-powered Air Compressor for use in a Small-scale Compressed Air Energy Storage System," M.S. thesis, Dept. of Mech. and Aero. Eng., Naval Postgraduate School.

[9]   International Energy Agency, 2018, "Global Energy and CO_2 Status Report, 2017." [Online]. Available: https://www.iea.org/publications/freepublications/ publication/GECO2017.pdf

[10]   United Nations Environment, 2018, "Executive Summary: The Emissions Gap Report 2017." [Online]. Available: https://unfccc.int/sites/default/files/resource/ 91_Emissions%20Gap%20Report_Talanoa_WAW.pdf

[11]   Berwyn, B., 2018, "IPCC: Radical Energy Transformation Needed to Avoid 1.5 Degrees Global Warming." [Online]. Available: https://insideclimatenews.org/ news/07102018/ipcc-climate-change-science-report-data-carbon-emissions-heat-waves-extreme-weather-oil-gas-agriculture

[12]   Enerdata, n.d., "Global Energy Trends, 2018 Edition. A Step Backward for the Energy Transition." [Online]. Available: https://www.enerdata.net/publications/reports-presentations/2018-world-energy-trends-projections.html

[13]   Union of Concerned Scientists, n.d., "Renewable Energy Can Provide 80 Percent of U.S. Electricity by 2050." [Online]. Available: https://www.ucsusa.org/clean_energy/smart-energy-solutions/increase-renewables/renewable-energy-80-percent-us-electricity.html#.XFY09fZFxrR

[14]   Stefan, P. and Lehmann, H., n.d., "Renewable Energy Outlook 2030 Energy Watch Group Global Renewables Energy Scenarios. Executive Summary." [Online]. Available: http://www.isusi.de/downloads/REO_2030_ExcecSummary_de.pdf

[15]   U.S. Department of Energy, n.d., "Revolution Now." [Online]. Available: https://www.energy.gov/revolution-now

[16]   Sabihuddin, S., Kiprakis, A. E. and Mueller, M., 2014, "A Numerical and graphical Review of Energy Storage Technologies," *Energies 2015*, 8, pp. 172–216.

[17]   John, J. S., 2017, "Global Energy Storage to Double 6 Times by 2030, Matching Solar's Spectacular Rise." [Online]. Available: https://www.greentechmedia.com/articles/read/global-energy-storage-double-six-times-by-2030-matching-solar-spectacular#gs.s3WmiHFF

[18]   Hart, D. M, Bonvillian, W. B. and Austin, N., 2018, "Energy Storage for the Grid:Policy Options for Sustaining Innovation." [Online]. Available: https://energy.mit.edu/wp-content/uploads/2018/04/Energy-Storage-for-the-Grid.pdf

[19]   Wang, J., et al., 2017, "Overview of Compressed Air Energy Storage and Technology Development." [Online]. Available: http://wrap.warwick.ac.uk/91858/7/WRAP-overview-compressed-air-energy-storage-technology-development-Wang-2017.pdf

[20]   Venkataramani, G., Ramalingam, V. and Viswanathan, K., 2018, "Harnessing Free Energy from Nature for Efficient Operation of Compressed Air Energy Storage System and Unlocking the Potential of Renewable Power Generation." [Online]. Available: https://www.nature.com/articles/s41598-018-28025-5

[21]   "Compressed Air Energy Storage," *Wikipedia*. Accessed 28 Aug. 2018. [Online]. https://en.wikipedia.org/wiki/Compressed_air_energy_storage

[22]   Manwell, J. F. and McGowan, J. G., 2018, "A Review of Utility Scale Energy Storage Options and Integration with Offshore Wind in Massachusetts." [Online]. Available: https://ag.umass.edu/sites/ag.umass.edu/files/projects/related-files/utility_scale_energy_storage_options_with_offshore_wind_umass_wind_energy_center_june_2018.pdf

[23]   RWE Power, n.d., "ADELE – Adiabatic Compressed-Air Energy Storage for Electricity Supply." [Online]. Available: https://www.rwe.com/web/cms/mediablob/en/391748/data/364260/1/rwe-power-ag/innovations/Brochure-ADELE.pdf

[24]   Tweed, C., 2015, "Toronto Hydro Pilots World's First Offshore Compressed-Air Energy Storage Project." [Online]. Available: https://www.greentechmedia.com/articles/read/toronto-hydro-pilots-worlds-first-offshore-compressed-air-energy-storage#gs.LZp1CgIF

[25]   Chen, H. S., et al., 2013, "Compressed Air Energy Storage." [Online]. Available: https://www.researchgate.net/publication/300495902_Compressed_Air_Energy_Storage

[26]   University of Birmingham, 2014, "Highview Cryogenic Storage Pilot Plant Arrives at the University of Birmingham." [Online]. Available: https://www.birmingham.ac.uk/university/colleges/eps/news/college/2014/Highview-Cryogenic-Storage-Pilot-Plant-Arrives-at-the-University-of-Birmingham.aspx

[27]   Castellani, B., et al., 2018, "Small-Scale Compressed Air Energy Storage Application for Renewable Energy Integration in a Listed Building." [Online]. Available: https://www.researchgate.net/publication/326558522_Small-Scale_Compressed_Air_Energy_Storage_Application_for_Renewable_Energy_Integration_in_a_Listed_Building

[28]   "Black Start," *Wikipedia*. Accessed 06 Feb. 2019. [Online]. https://en.wikipedia.org/wiki/Black_start

[29]   Naval Education and Training Professional Development and Technology Center, n.d., "Gas Turbine Systems Technician (Electrical) 3/ Gas Turbine Systems Technician (Mechanical) 3, Volume 2," http://www.navybmr.com/study%20material/NAVEDTRA%2014114.pdf

[30]   LEONICS, n.d., "Basics of MPPT Solar Charge Controller." [Online]. Available: http://www.leonics.com/support/article2_14j/articles2_14j_en.php

[31]   MidNite Solar, n.d., "Classic MPPT Solar Charge Controller." [Online]. Available: http://www.midnitesolar.com/pdfs/theClassics.pdf

[32] Wikipedia, n.d., "Supercapacitor." [Online]. Available: https://en.wikipedia.org/wiki/Supercapacitor

[33] Maxwell, n.d., "Product Specifications." [Online]. Available: http://www.maxwell.com/images/documents/56vmodule_ds_1017119-3.pdf

[34] SMA, n.d., "Sunny Island 4548-US." [Online]. Available: http://files.sma.de/dl/15216/SUNNYIS4548_6048US-DUS161422W.pdf

[35] Balsamico, A., 2019, "PLCs vs PC-Based Controls." [Online]. Available: https://info.panelshop.com/blog/plcs-vs.-pc-bas-controls

[36] Allen-Bradley User Manual, n.d., "Micro830, Micro850, Micro870 Programmable Controllers." [Online]. Available: https://literature.rockwellautomation.com/idc/groups/literature/documents/um/2080-um002_-en-e.pdf

[37] BK Precision, n.d., "Switching DC Bench Power Supply with USB Charger Output 1-36V, 0-3A." [Online]. Available: http://www.bkprecision.com/products/power-supplies/1550-switching-dc-bench-power-supply-with-usb-charger-output-1-36v-0-3a.html

[38] Rockwell Automation, n.d., "Connected Components Workbench Software Quick Tips." [Online]. Available: https://literature.rockwellautomation.com/idc/groups/literature/documents/sp/9328-sp002_-en-p.pdf

[39] Allen-Bradley User Manual, n.d., "Connected Components Workbench Software Guide for Studio 5000 Logix Designer Software Users." [Online]. Available: https://literature.rockwellautomation.com/idc/groups/literature/documents/qr/9328-qr001_-en-e.pdf

[40] Rockwell Automation, n.d., "L12-Basic PLC Programming with Micro800 Controllers and Panelview 800 Graphic Terminal." [Online]. Available: https://www.rockwellautomation.com/resources/downloads/rockwellautomation/noa/RAOTM%20Lab%20Manuals/L12-manual.pdf

[41] Rockwell Automation, n.d., "Micro800 Programming Basics Tutorial 2: Variables and Instruction Blocks." [Online]. Available: https://www.brightonk12.com/cms/lib/MI02209968/Centricity/Domain/517/Tutorial%2002%20PLC.pdf

INITIAL DISTRIBUTION LIST

1.   Defense Technical Information Center
        Ft. Belvoir, Virginia

2.   Dudley Knox Library
        Naval Postgraduate School
        Monterey, California